

Implications of Flavor Symmetries for Baryon Number Violation

Arnau Bas i Beneito,^{1,*} Ajdin Palavrić,^{1,2,†} and Andrea Sainaghi^{3,4,5,‡}

¹*Institut de Física Corpuscular (IFIC), Consejo Superior de Investigaciones Científicas (CSIC) and Universitat de València (UV), 46980 València, Spain*

²*Department of Physics, University of Basel, Klingelbergstrasse 82, CH-4056 Basel, Switzerland*

³*Istituto Nazionale di Fisica Nucleare, Sezione di Padova, 35131 Padova, Italy*

⁴*Dipartimento di Fisica e Astronomia "Galileo Galilei", Università di Padova, 35131 Padova, Italy*

⁵*Physik-Institut, Universität Zürich, CH-8057 Zürich, Switzerland*

In the Standard Model, baryon number is an accidental symmetry, whose violation would constitute unambiguous evidence of new physics, with proton decay providing its most prominent experimental signature. At the same time, the peculiar structure of flavor can serve as a guiding principle for exploring possible new-physics effects. In this work, we present a systematic classification of dimension-six baryon-number-violating (BNV) SMEFT operators across several flavor-symmetry assumptions and analyze the resulting phenomenology. Interestingly, in certain flavor scenarios the non-trivial interplay with tiny neutrino masses leads to proton-decay constraints compatible with BNV scales in the multi-TeV range. Finally, we complement the EFT analysis by identifying one-particle UV completions of the BNV operators, revealing scenarios in which the leading-order EFT description may not fully account for their underlying dynamics.

I. INTRODUCTION

One of the most striking features of the Standard Model (SM) is the intricate pattern of fermion masses and mixings that defines its flavor structure. In the absence of Yukawa interactions, the SM would exhibit an extensive global flavor symmetry allowing independent unitary rotations among the three generations of quarks and leptons. The introduction of the Yukawa couplings explicitly breaks this symmetry, giving rise to the observed hierarchies and to the principal sources of flavor and CP violation within the SM. Framing the flavor structure in terms of this approximate global symmetry clarifies the origin of the observed hierarchies and provides a systematic guide for constructing extensions of the SM consistent with flavor constraints.

The Minimal Flavor Violation (MFV) framework [1, 2], originally developed in the quark sector, provides a symmetry-based strategy for addressing the flavor problem associated with TeV-scale new physics. MFV posits that the only sources of flavor and CP violation are the Yukawa couplings, which explicitly break the SM flavor symmetry. By promoting these Yukawa matrices to spurionic fields with definite transformation properties, one ensures that any higher-dimensional operator or new-physics interaction respects the SM flavor alignment. Consequently, new-physics effects acquire CKM-like suppression factors through structures such as $Y_u Y_u^\dagger$ and $Y_d Y_d^\dagger$, thereby mitigating potentially dangerous FC-NCs and CP-violating contributions and ensuring compatibility with precision measurements in kaon, B -meson, and D -meson systems.

Building on this quark-sector construction, the MFV framework was later generalized to the lepton sector [3–6] to accommodate neutrino mass generation and to analyze charged-lepton flavor violation (cLFV). In this context, processes such as $\mu \rightarrow e\gamma$ and $\mu \rightarrow 3e$ remain controlled by the same spurionic structures that dictate flavor breaking in the SM, ensuring the characteristic MFV suppression. The framework naturally interfaces with seesaw scenarios [7–9], where lepton-number violation (LNV) introduces additional breaking of the flavor symmetry in the neutrino sector.

While MFV was initially developed to address the flavor problem in the quark and lepton sectors, the same organizing principle has been applied in a variety of broader contexts. A notable application is found in leptoquark frameworks, where flavor covariance of the new interactions can be ensured either by introducing appropriate spurion fields or by allowing the leptoquarks to transform nontrivially under the flavor symmetry [10]. Beyond the leptoquark models, MFV has also been explored in scenarios featuring baryon-number violation (BNV). The embedding of MFV within supersymmetric models has been shown to suppress proton-decay operators to levels consistent with experimental bounds, thereby removing the need for imposing R -parity [11]. The potential correlation between LNV and proton stability was later investigated, suggesting that the smallness of neutrino masses and the longevity of the proton may originate from a common symmetry-breaking pattern, potentially allowing the BNV scale to lie near the TeV regime [12]. This possibility was subsequently revisited within a broader effective field theory (EFT) framework [13].

Focusing more directly on the BNV sector, proton decay plays a central role among low-energy probes of physics beyond the SM [14–17]. Its observation would provide unambiguous evidence for BNV interactions, while the continued absence of a signal places exceptionally stringent limits on such dynamics. More concretely,

* arnau.bas@ific.uv.es

† ajdin.palavric@ific.uv.es

‡ andrea.sainaghi@phd.unipd.it

current searches by Super-Kamiokande (Super-K) constrain the proton lifetime to the level of $10^{32} - 10^{33}$ years for many decay channels [18–20], with the most sensitive modes, such as $p \rightarrow \pi^0 e^+$, already setting lower limits exceeding 10^{34} years. Future experiments, including Hyper-Kamiokande (Hyper-K) [21] and DUNE [22], are expected to substantially improve proton-decay sensitivities, with projected reach up to lifetimes of $\mathcal{O}(10^{35})$ years in selected channels after several years of data taking. Interpreted within the Standard Model EFT (SMEFT) framework [23, 24], these bounds translate into extremely high scales for the dimension-six BNV operators, reaching up to $\Lambda_B \sim \mathcal{O}(10^{16} \text{ GeV})$ in the anarchic limit [25]. Additional constraints arise from direct searches for BNV processes at colliders involving heavy quarks [26–28], but these are negligible compared to the limits set by proton stability. Proton-decay limits therefore dominate the phenomenology of all SMEFT BNV operators, including those contributing only at loop level or via multi-body final states [29–36]. This pronounced suppression of BNV interactions involving light-family fermions thus provides a compelling motivation to treat the BNV sector within a flavor-oriented framework, in line with the MFV considerations introduced above.

In this paper, we investigate the implications of embedding BNV and LNV within well-defined flavor frameworks. Our primary analysis is carried out in an *extended* MFV scenario, in which both Yukawa couplings and neutrino masses serve as the spurions breaking the underlying symmetry. In addition, we explore several alternative flavor symmetries to compare their predictions with the ones obtained assuming MFV, particularly those in which new physics couples preferentially to third-generation fermions [37–40]. Concentrating on the four dimension-six BNV operators of the SMEFT, we construct their flavor-invariant combinations and identify the least suppressed structures. This allows for a quantitative comparison between the characteristic scales governing BNV and LNV processes. To complement the EFT analysis, we also examine ultraviolet (UV) completions that generate these operators at tree level, allowing us to assess the corresponding phenomenological implications within and beyond the EFT description.

The remainder of this work is organized as follows. In Sec. II, we provide an overview of the extended MFV framework, outlining the relevant spurion structures, with particular emphasis on the inclusion of neutrino mass effects. In Sec. III, we perform the EFT analysis by constructing the flavor invariants associated with the four dimension-six BNV SMEFT operators and identifying the least suppressed combinations, followed by a discussion of their phenomenological implications. Sec. IV is devoted to the UV completions that can generate these operators, establishing connections between the low-energy EFT and possible high-scale dynamics. In Sec. V, we explore alternative flavor frameworks built on smaller symmetry groups and discuss their implications. Finally, Sec. VI summarizes our findings and presents the

conclusions. Additional technical details and derivations are collected in the appendices.

II. OVERVIEW OF THE EXTENDED MFV

The gauge interactions of the SM are invariant under a large global flavor symmetry in the limit where all Yukawa couplings vanish. This symmetry corresponds to independent unitary transformations acting on each type of fermion field, leading to the maximal flavor group

$$G_F \equiv U(3)^5 = U(3)_q \times U(3)_u \times U(3)_d \times U(3)_\ell \times U(3)_e, \quad (1)$$

where the five $U(3)$ factors correspond to independent unitary rotations of the left-handed quark doublets (q), right-handed up-type quarks (u), right-handed down-type quarks (d), left-handed lepton doublets (ℓ), and right-handed charged leptons (e), respectively. The transformation properties of the SM fermions under G_F are given by

$$\begin{aligned} q &\sim (\mathbf{3}, \mathbf{1}, \mathbf{1}, \mathbf{1}, \mathbf{1}) \equiv \mathbf{3}_q, & \ell &\sim (\mathbf{1}, \mathbf{1}, \mathbf{1}, \mathbf{3}, \mathbf{1}) \equiv \mathbf{3}_\ell, \\ u &\sim (\mathbf{1}, \mathbf{3}, \mathbf{1}, \mathbf{1}, \mathbf{1}) \equiv \mathbf{3}_u, & e &\sim (\mathbf{1}, \mathbf{1}, \mathbf{1}, \mathbf{1}, \mathbf{3}) \equiv \mathbf{3}_e. \\ d &\sim (\mathbf{1}, \mathbf{1}, \mathbf{3}, \mathbf{1}, \mathbf{1}) \equiv \mathbf{3}_d, \end{aligned} \quad (2)$$

The only interaction terms in the Standard Model Lagrangian that explicitly break G_F are the Yukawa couplings

$$-\mathcal{L}_Y = \bar{q}_p [Y_d]^p{}_r d^r H + \bar{q}_p [Y_u]^p{}_r u^r \tilde{H} + \bar{\ell}_p [Y_e]^p{}_r e^r H + \text{h.c.}, \quad (3)$$

where H denotes the Higgs doublet and $\tilde{H} = i\sigma_2 H^*$. Throughout this work, we retain explicit flavor indices and use a covariant index notation, making G_F transformations manifest and streamlining the construction of invariants.

The MFV framework [1] formalizes the idea that the flavor-breaking structure of the SM persists even in the presence of new physics. This is achieved by promoting the Yukawa matrices to spurion fields that transform under G_F in such a way that the full Lagrangian, including higher-dimensional operators, remains formally invariant. The transformation properties of the spurions are defined such that the Yukawa interaction terms become formally invariant under G_F :

$$\begin{aligned} Y_d &\sim (\mathbf{3}, \mathbf{1}, \bar{\mathbf{3}}, \mathbf{1}, \mathbf{1}) \equiv (\mathbf{3}_q, \bar{\mathbf{3}}_d), \\ Y_u &\sim (\mathbf{3}, \bar{\mathbf{3}}, \mathbf{1}, \mathbf{1}, \mathbf{1}) \equiv (\mathbf{3}_q, \bar{\mathbf{3}}_u), \\ Y_e &\sim (\mathbf{1}, \mathbf{1}, \mathbf{1}, \mathbf{3}, \bar{\mathbf{3}}) \equiv (\mathbf{3}_\ell, \bar{\mathbf{3}}_e). \end{aligned} \quad (4)$$

The MFV hypothesis asserts that these three spurions, in absence of neutrino masses, govern all flavor-violating interactions, both in the SM and in any effective extension, i.e. any higher-dimensional operator that violates flavor must do so through insertions of Y_d , Y_u , or Y_e , arranged to preserve invariance under G_F . This reasoning applies naturally to the SMEFT framework, where MFV

provides a symmetry-based principle that constrains the flavor structure of higher-dimensional operators. It ensures that all such operators respect the same flavor-breaking pattern as the SM itself, thus providing a controlled and phenomenologically consistent extension of the low-energy theory [41–43].

While the MFV framework successfully reproduces the flavor-breaking pattern of the SM in the limit of massless neutrinos, its minimal implementation fails to accommodate the observed lepton-flavor violation (LFV) implied by neutrino oscillations [44]. In the absence of right-handed neutrinos or Majorana mass terms, the SM lepton sector contains a single flavor-breaking spurion, the charged-lepton Yukawa matrix Y_e , which breaks the global $U(3)_\ell \times U(3)_e$ symmetry. Introducing neutrino masses necessarily requires new spurions in order to formally restore the flavor symmetry.

Focusing on the EFT framework, we consider neutrino masses generated by the dimension-five Weinberg operator [14]¹

$$[\mathcal{O}_W]_{pr} = (\bar{\ell}_p \tilde{H})(\tilde{H}^\dagger \ell_r^c), \quad (5)$$

where \mathcal{O}_W violates total lepton number by two units and induces a Majorana mass term for the left-handed neutrinos after Electroweak Symmetry Breaking (EWSB). In addition, with lepton doublets transforming as $\ell \sim \mathbf{3}_\ell$ under the MFV assumption, the Weinberg operator explicitly breaks the flavor symmetry. To restore invariance under the flavor symmetry, the coefficient of the operator must be promoted to a spurion field that transforms appropriately under $U(3)_\ell$. Since the operator in Eq. (5) involves the tensor product of the form

$$\bar{\ell} \ell^c \sim \bar{\mathbf{3}}_\ell \otimes \bar{\mathbf{3}}_\ell = \bar{\mathbf{6}}_\ell \oplus \mathbf{3}_\ell, \quad (6)$$

the Weinberg operator selects out the symmetric part of this decomposition, and thus requires the introduction of a symmetric spurion Υ_ν , transforming as

$$\Upsilon_\nu \sim (\mathbf{1}, \mathbf{1}, \mathbf{1}, \mathbf{6}, \mathbf{1}) \equiv \mathbf{6}_\ell. \quad (7)$$

This additional spurion encodes the flavor-breaking effects associated with Majorana neutrino masses and represents the minimal extension of the lepton flavor sector beyond the charged lepton Yukawa coupling within the MFV framework [3].

The flavor-invariant interaction term can then be written as

$$\mathcal{L}_{\text{SMEFT}} \supset -\frac{1}{2\Lambda_L} [\Upsilon_\nu]^{pr} (\bar{\ell}_p \tilde{H})(\tilde{H}^\dagger \ell_r^c) + \text{h.c.}, \quad (8)$$

where Λ_L denotes the LNV scale. Upon EWSB, this interaction term gives rise to a Majorana mass term for the left-handed neutrinos

$$\mathcal{L}_\nu \supset -\frac{1}{2} [m_\nu]^{pr} (\bar{\nu}_p \nu_r^c) + \text{h.c.}, \quad [m_\nu]^{pr} = \frac{v^2}{2\Lambda_L} [\Upsilon_\nu]^{pr}, \quad (9)$$

where the Higgs vacuum expectation value is taken to be $\langle H \rangle = \frac{1}{\sqrt{2}} [0 \ v]^\top$. In this *extended* MFV setup, characterized by Y_e and Υ_ν spurions, one may exploit the $U(3)_\ell \times U(3)_e$ flavor symmetry to bring the charged lepton Yukawa matrix into a convenient form. Specifically, by performing unitary transformations

$$\ell \rightarrow V_\ell \ell, \quad e \rightarrow V_e e, \quad V_{\ell,e} \in U(3)_{\ell,e}, \quad (10)$$

the matrix Y_e can be brought to the diagonal form

$$Y_e \rightarrow \widehat{Y}_e = V_\ell^\dagger Y_e V_e, \quad \widehat{Y}_e = \sqrt{2} \frac{\widehat{m}_e}{v}, \quad (11)$$

which fixes the V_ℓ and V_e rotations. After EWSB, the neutrino mass matrix m_ν in Eq. (9) can be diagonalized by a single unitary matrix U_ν :

$$m_\nu \rightarrow \widehat{m}_\nu = U_\nu^\dagger m_\nu U_\nu^*, \quad (12)$$

which can be used to express Υ_ν as

$$\Upsilon_\nu \rightarrow \frac{2\Lambda_L}{v^2} U_\nu \widehat{m}_\nu U_\nu^\dagger. \quad (13)$$

In this basis, where the charged lepton Yukawa matrix Y_e is diagonal, the unitary matrix U_ν that diagonalizes the neutrino mass matrix coincides with the leptonic mixing matrix, i.e. we directly identify $U_\nu = U_{\text{PMNS}}$, which governs neutrino oscillations through its appearance in the charged-current interactions.² This relation allows us to express the spurion Υ_ν directly in terms of the physical neutrino masses and mixing angles. Eq. (13) can further be expressed in its component form as

$$[\Upsilon_\nu]_{ij} = \frac{2\Lambda_L}{v^2} \sum_k [U_\nu]_{ik} [U_\nu]_{jk} \widehat{m}_{\nu,k}, \quad (14)$$

which can be used to analyze the parametrization of Υ_ν depending on the mass ordering. In addition, the Majorana phases in the PMNS matrix are neglected, as they do not influence the operator structures relevant for our analysis. Given the unknown absolute neutrino mass scale, we derive analytical approximations for Υ_ν in the normal (NO) and inverted (IO) ordering by expanding around the lightest neutrino mass, employing the known

¹ The charge-conjugated field ψ^c is defined as $\psi^c \equiv C\bar{\psi}^\dagger$, where C is the charge-conjugation matrix. In two-component (Weyl) notation, the charge-conjugated fields are defined as $\psi_L^c \equiv -i\sigma_2 \psi_L$ and $\psi_R^c = i\sigma_2 \psi_R$.

² If we chose not to use the $U(3)_\ell \times U(3)_e$ flavor rotations to diagonalize the charged lepton Yukawa matrix Y_e , then the leptonic mixing matrix appearing in the charged current would take slightly modified form given by $U_{\text{PMNS}} = V_\ell^\dagger U_\nu$.

mass-squared splittings and mixing parameters. As input, we adopt the central values from the most recent global fit to neutrino-oscillation data [44].

Normal ordering (NO). In the case of normal ordering, where $\hat{m}_{\nu,1} < \hat{m}_{\nu,2} < \hat{m}_{\nu,3}$, the experimentally measured parameters that can be used are the mass-squared splittings

$$\Delta m_{21}^2 = \hat{m}_{\nu,2}^2 - \hat{m}_{\nu,1}^2, \quad \Delta m_{32}^2 = \hat{m}_{\nu,3}^2 - \hat{m}_{\nu,2}^2. \quad (15)$$

Assuming $\hat{m}_{\nu,1} \ll \hat{m}_{\nu,2} \ll \hat{m}_{\nu,3}$, we expand the neutrino masses in terms of the heavier eigenvalues using

$$\begin{aligned} \hat{m}_{\nu,3} &\approx \sqrt{\Delta m_{32}^2 + \Delta m_{21}^2} \approx \sqrt{\Delta m_{32}^2} + \frac{\Delta m_{21}^2}{2\sqrt{\Delta m_{32}^2}} + \dots, \\ \hat{m}_{\nu,2} &\approx \sqrt{\Delta m_{21}^2}, \end{aligned} \quad (16)$$

which, once plugged into Eq. (14), yields

$$\begin{aligned} [\Upsilon_\nu]_{ij} &\approx \frac{2\Lambda_L}{v^2} \left[\delta_{ij} \sqrt{\Delta m_{21}^2} - [U_\nu]_{i1} [U_\nu]_{j1} \sqrt{\Delta m_{21}^2} \right. \\ &\quad \left. + [U_\nu]_{i3} [U_\nu]_{j3} \left(\sqrt{\Delta m_{32}^2} - \sqrt{\Delta m_{21}^2} \right) \right. \\ &\quad \left. + \mathcal{O} \left(\Delta m_{21}^2 / \sqrt{\Delta m_{32}^2} \right) \right]. \end{aligned} \quad (17)$$

Inverted ordering (IO). For the inverted mass ordering, where $m_{\nu,3} < m_{\nu,1} < m_{\nu,2}$, it is convenient to express the mass-squared splittings as

$$\begin{aligned} \Delta m_{23}^2 &= \hat{m}_{\nu,2}^2 - \hat{m}_{\nu,3}^2, \\ \Delta m_{13}^2 &= \hat{m}_{\nu,1}^2 - \hat{m}_{\nu,3}^2 = \Delta m_{23}^2 - \Delta m_{21}^2. \end{aligned} \quad (18)$$

Assuming $\hat{m}_{\nu,3} \ll \hat{m}_{\nu,1}, \hat{m}_{\nu,2}$, we expand around $\hat{m}_{\nu,3}$, and, once again, rewrite the heavier masses in terms of $\sqrt{\Delta m_{13}^2}$ and $\sqrt{\Delta m_{23}^2}$. The resulting parametrization for Υ_ν is then given as

$$\begin{aligned} [\Upsilon_\nu]_{ij} &\approx \frac{2\Lambda_L}{v^2} \left[[U_\nu]_{i1} [U_\nu]_{j1} \sqrt{\Delta m_{13}^2} \right. \\ &\quad \left. + [U_\nu]_{i2} [U_\nu]_{j2} \sqrt{\Delta m_{23}^2} + \mathcal{O}(\hat{m}_{\nu,3}) \right]. \end{aligned} \quad (19)$$

III. EFT ANALYSIS AND PHENOMENOLOGY

Building on the framework introduced in Sec. II, we now analyze the flavor-invariant structures of the dimension-six BNV SMEFT operators. Our goal is to systematically construct the minimal spurion insertions required to render these operators invariant under the full flavor symmetry group and to identify the dominant phenomenological channels associated with each structure. Throughout this analysis, we assume a hierarchical separation of scales, $\Lambda_L \gtrsim \Lambda_F \gg \Lambda_B$, where Λ_F characterizes flavor-symmetry breaking. This hierarchy allows

us to treat the spurions as background fields that can be consistently inserted when constructing BNV operators, whose UV dynamics occur at the scale Λ_B . This analysis establishes a framework for quantitatively linking the effective scales of BNV and LNV within the extended MFV scenario. For completeness, in App. B we also apply this formalism to the relevant cLFV transitions, illustrating their structure and suppression patterns within the same framework.

A. Flavor-Invariant BNV Structures

The non-observation of proton decay places extremely stringent lower limits on the scale suppressing BNV operators, typically requiring $\Lambda_B \gtrsim 10^{16}$ GeV for generic, unsuppressed flavor structures [25]. However, when the flavor symmetry is imposed, the structure of these operators becomes highly constrained: all sources of flavor breaking must arise through spurion insertions built from the known fermion mass matrices and mixing parameters. This naturally raises the question of whether such flavor-induced suppression can relax the lower bound on Λ_B , potentially bringing BNV phenomena even within the reach of current or future experiments.

To quantify the impact of flavor symmetries on BNV processes, we proceed with the analysis of the flavor invariants, with particular emphasis placed on the role of Υ_ν , which opens up the novel possibilities for constructing invariant structures. For each operator, we identify the transformation properties of the fermion bilinears under the flavor group G_F and construct the minimal set of spurion insertions required to restore flavor invariance. In this construction, it is convenient to define the following composite spurionic tensors in the lepton sector

$$\begin{aligned} [\mathcal{T}_\ell]_s &\equiv \varepsilon_{prs} [Y_e Y_e^\dagger \Upsilon_\nu]^{rp} \sim \bar{\mathbf{3}}_\ell, \\ [\mathcal{T}_e]_t &\equiv \varepsilon_{prs} [Y_e Y_e^\dagger \Upsilon_\nu]^{rp} [Y_e]_s^s [Y_e]_t^t \sim \bar{\mathbf{3}}_e. \end{aligned} \quad (20)$$

Additional group-theoretical aspects of the flavor-invariant construction and the associated numerical values are provided in App. A. The resulting flavor-invariant structures are summarized in Tab. 1, which lists the four independent dimension-six BNV SMEFT operators together with their minimal spurion insertions under the extended MFV framework. As a notational convention, the SMEFT Wilson coefficients are denoted by \mathcal{C} .

Several symmetry properties of the operators directly determine their phenomenological relevance. For example, at the lowest non-vanishing order in the spurion expansion, $[\mathcal{C}_{duue}]_{prst}$ is antisymmetric under $r \leftrightarrow s$, which prevents this operator from mediating tree-level two-body proton decay [46, 47]. Likewise, the nominally leading spurion structure $[\mathcal{C}_{qque}]_{prst} \sim \varepsilon_{prx} [Y_u]_s^x [\mathcal{T}_e]_t$ vanishes since $[\mathcal{O}_{qque}]^{prst}$ is symmetric under $p \leftrightarrow r$ and, as a result, the first non-vanishing flavor-invariant structure arises only at higher order in the spurion expansion.

Another particularly illustrative example is provided by the operator \mathcal{O}_{qqql} , whose flavor structure is subject

Operator	Definition	Spurion expansion	Order
$[\mathcal{O}_{qqq\ell}]^{prst}$	$\varepsilon_{\alpha\beta\gamma}[i\sigma_2]_{\dot{a}\dot{d}}[i\sigma_2]_{\dot{b}\dot{e}}(\bar{q}^{c\alpha,p}q^{\beta,b,r})(\bar{q}^{c\gamma,\dot{e},s}\ell^{\dot{d},t})$	$\frac{1}{\Lambda_B^2}\{\varepsilon_{prx}[Y_u Y_u^\dagger]^x_s + \varepsilon_{pxs}[Y_u Y_u^\dagger]^x_r + \varepsilon_{xrs}[Y_u Y_u^\dagger]^x_p\}[\mathcal{T}_\ell]_t$	$\mathcal{O}(Y_e^2\Upsilon_\nu)$
$[\mathcal{O}_{duq\ell}]^{prst}$	$\varepsilon_{\alpha\beta\gamma}(\bar{d}^{c\alpha,p}u^{\beta,r})(\bar{q}^{c\gamma,s}i\sigma_2\ell^t)$	$\frac{1}{\Lambda_B^2}\varepsilon_{abs}[Y_u]^a_r[Y_d]^b_p[\mathcal{T}_\ell]_t$	$\mathcal{O}(Y_u Y_d Y_e^2\Upsilon_\nu)$
$[\mathcal{O}_{qque}]^{prst}$	$\varepsilon_{\alpha\beta\gamma}(\bar{q}^{c\alpha,p}i\sigma_2q^{\beta,r})(\bar{u}^{c\gamma,s}e^t)$	$\frac{1}{2\Lambda_B^2}\{\varepsilon_{abp}[Y_u Y_u^\dagger]^b_r + \varepsilon_{abr}[Y_u Y_u^\dagger]^b_p\}[Y_u]^a_s[\mathcal{T}_e]_t$	$\mathcal{O}(Y_u^3 Y_e^3 \Upsilon_\nu)$
$[\mathcal{O}_{duee}]^{prst}$	$\varepsilon_{\alpha\beta\gamma}(\bar{d}^{c\alpha,p}u^{\beta,r})(\bar{u}^{c\gamma,s}e^t)$	$\frac{1}{\Lambda_B^2}\varepsilon_{ars}[Y_u^\dagger Y_d]^a_p[\mathcal{T}_e]_t$	$\mathcal{O}(Y_u Y_d Y_e^3 \Upsilon_\nu)$

TABLE 1. Overview of the dimension-six BNV SMEFT operators and the flavor-invariant structures in the extended MFV framework. The first column lists the relevant operator structures, while the second gives their definitions in terms of SM fermion fields. The third column displays the minimal spurion insertions required to render each operator invariant under the full flavor symmetry group G_F , expressed in terms of the SM Yukawa matrices and the additional Υ_ν spurion. The final column reports the overall suppression order in spurions, highlighting the flavor-breaking structure induced by the extended MFV hypothesis. The constructions account for Fierz identities, permutation symmetries, and charge-conjugation conventions, with the goal of identifying the least suppressed, non-vanishing flavor-invariant structures relevant for BNV processes. In the operator definitions, Greek indices α, β, γ label $SU(3)_C$, Latin dotted indices $\dot{a}, \dot{b}, \dot{d}, \dot{e}$ denote $SU(2)_L$, and p, r, s, t represent flavor indices. In the spurion expansions, all indices are understood to refer to flavor. Symmetry relations, arising from the Fierz identities and the permutation symmetries, can be found in Ref. [45].

Operator	Definition	Tree-level matching
$[\mathcal{O}_{udd}^{S,LL}]_{prst}$	$\varepsilon_{\alpha\beta\gamma}(\bar{u}_{L,p}^{c,\alpha}d_{L,r}^\beta)(\bar{d}_{L,s}^{c,\gamma}\nu_{L,t})$	$[\mathcal{C}_{qqq\ell}]_{srpt} - [\mathcal{C}_{qqq\ell}]_{rpst} + [\mathcal{C}_{qqq\ell}]_{prst}$
$[\mathcal{O}_{duu}^{S,LL}]_{prst}$	$\varepsilon_{\alpha\beta\gamma}(\bar{d}_{L,p}^{c,\alpha}u_{L,r}^\beta)(\bar{u}_{L,s}^{c,\gamma}e_{L,t})$	$[\mathcal{C}_{qqq\ell}]_{srpt} - [\mathcal{C}_{qqq\ell}]_{rspt} + [\mathcal{C}_{qqq\ell}]_{rpst}$
$[\mathcal{O}_{duu}^{S,LR}]_{prst}$	$\varepsilon_{\alpha\beta\gamma}(\bar{d}_{L,p}^{c,\alpha}u_{L,r}^\beta)(\bar{u}_{R,s}^{c,\gamma}e_{R,t})$	$-[\mathcal{C}_{qque}]_{prst} - [\mathcal{C}_{qque}]_{rpst}$
$[\mathcal{O}_{duu}^{S,RL}]_{prst}$	$\varepsilon_{\alpha\beta\gamma}(\bar{d}_{L,p}^{c,\alpha}u_{R,r}^\beta)(\bar{u}_{L,s}^{c,\gamma}e_{L,t})$	$[\mathcal{C}_{duq\ell}]_{prst}$
$[\mathcal{O}_{dud}^{S,RL}]_{prst}$	$\varepsilon_{\alpha\beta\gamma}(\bar{d}_{R,p}^{c,\alpha}u_{R,r}^\beta)(\bar{d}_{L,s}^{c,\gamma}\nu_{L,t})$	$-[\mathcal{C}_{duq\ell}]_{prst}$
$[\mathcal{O}_{dud}^{S,RR}]_{prst}$	$\varepsilon_{\alpha\beta\gamma}(\bar{d}_{R,p}^{c,\alpha}u_{R,r}^\beta)(\bar{u}_{R,s}^{c,\gamma}e_{R,t})$	$[\mathcal{C}_{duee}]_{prst}$

TABLE 2. Dimension-six $\Delta B = \Delta L = 1$ operators in the LEFT and their corresponding tree-level matching to the SMEFT basis. The matching coefficients are presented without specifying a particular flavor basis; the basis choice and transformation to the up/down mass basis are discussed in the main text.

to nontrivial permutation relations among its quark indices. As shown in Ref. [45], the corresponding Wilson coefficient decomposes into independent components with fully antisymmetric (A), fully symmetric (S), and mixed (M) flavor structures. In the spurion expansion, these components contribute at different orders, and in our EFT analysis we retain only the leading flavor invariants, namely those requiring the minimal number of spurion insertions. The fully antisymmetric component yields an $\mathcal{O}(1)$ invariant without any spurion insertions, while the next-to-leading contribution arises from an insertion of the form $Y_u Y_u^\dagger$, leading to structures of the type $\mathcal{C}_{prst} \sim \varepsilon_{prx}[Y_u Y_u^\dagger]^x_s[\mathcal{T}_\ell]_t$ [12]. These contributions, however, must satisfy the intrinsic flavor-operator identity [16]

$$[\mathcal{O}_{qqq\ell}]^{prst} + [\mathcal{O}_{qqq\ell}]^{rpst} = [\mathcal{O}_{qqq\ell}]^{srpt} + [\mathcal{O}_{qqq\ell}]^{sppt}, \quad (21)$$

which enforces a definite symmetry of the Wilson coeffi-

cient. Imposing this condition yields

$$\mathcal{C}_{prst} \sim \{\varepsilon_{prx}[Y_u Y_u^\dagger]^x_s - (p \leftrightarrow s) - (r \leftrightarrow s)\}[\mathcal{T}_\ell]_t, \quad (22)$$

which, like the spurion-free contribution, is fully anti-symmetric under all index permutations. Thus, the leading invariants selected in our analysis correspond to well-defined symmetry components of the coefficient, and, as we show in the phenomenological section, their numerical impact is parametrically comparable to that of the nominal $\mathcal{O}(1)$ term.

Given these structural features, it is worth highlighting that previous work, most notably Ref. [12], provided an important first exploration of MFV assumption applied to BNV operators offering valuable insight into how flavor symmetries shape the corresponding interactions. Since it was carried out prior to the development of the modern SMEFT framework, improved determinations of hadronic matrix elements, and the current precision in neutrino data, our present analysis is able to revisit and extend those results within a fully consistent spurion decomposition. This allows us to make the symmetry structure of dimension-six BNV operators explicit and to identify the complete set of non-vanishing flavor-invariant contributions.

B. Phenomenology of BNV Operators

1. Methodology

With the complete set of minimal spurion structures identified, we now turn to the phenomenological analysis of the BNV operators. We first perform the tree-level SMEFT-LEFT matching for the relevant dimension-six BNV operators. At the electroweak scale, with the heavy

degrees of freedom integrated out, SMEFT operators collected in Tab. 1 match onto a corresponding set of four-fermion operators in the low-energy effective theory (LEFT). The resulting LEFT Lagrangian contains the leading $\Delta B = \Delta L = 1$ structures mediating proton decay [48, 49]. The explicit operator definitions, together with their corresponding tree-level matching relations, are collected in Tab. 2. Once again, as a notational convention, the LEFT Wilson coefficients are denoted by L .

In addition, the explicit form of the SMEFT-LEFT matching relations depends on the choice of flavor basis, which determines how the fermion fields are rotated to their mass eigenstates after electroweak symmetry breaking. In the quark sector, one may work either in the up or down basis, with the two choices being related by CKM rotations of the left-handed quark fields:

$$\text{up : } d_{L,p} \rightarrow V_{pr} d_{L,r}, \quad \text{down : } u_{L,p} \rightarrow V_{pr}^\dagger u_{L,r}, \quad (23)$$

where V denotes the CKM matrix. Consequently, the CKM matrix elements enter the flavor contractions of the BNV operators differently depending on the chosen basis. As input for quark masses and CKM parameters, we use the most recent PDG values [50]. In the remainder of the phenomenological analysis, we consider both arrangements to illustrate how the resulting CKM insertions affect the phenomenological predictions, in particular the relative magnitudes of the decay widths associated with different BNV channels.

Moving forward, in order to perform the computation of nucleon decay rates, the effective four-fermion inter-

actions derived in the LEFT must be further matched onto hadronic degrees of freedom at low energies, where quarks and gluons are replaced by baryons and mesons. This matching is performed within the framework of baryon chiral perturbation theory ($B\chi$ PT), which provides a systematic low-energy expansion of QCD [25, 51]. The quark-level BNV operators are thus translated into hadronic operators involving nucleon and meson fields, parameterized by a small number of low-energy constants that encode non-perturbative QCD dynamics, which are determined from lattice QCD calculations or phenomenological fits. In particular, for the nucleon decay channels relevant to our analysis, parity conservation of the strong interactions and isospin symmetry imply that only two independent nucleon matrix elements contribute.³

For the derivation of the proton-decay bounds, which constitute the main results of this work, we employ the experimental lower limits on the relevant two-body proton-decay channels as reported in Table 1 of Ref. [25]. While our numerical analysis covers all accessible two-body nucleon decay channels into pseudoscalar mesons and anti-lepton states, the dominant experimental constraints stem from the $p \rightarrow K^+ \nu_r$, $p \rightarrow \pi^0 \ell_r^+$, and $p \rightarrow K^0 \ell_r^+$ modes. When evaluated within the extended MFV framework, these channels provide the strongest sensitivity to the BNV operators considered in this work. For these modes, we present analytical expressions for the partial decay widths in terms of the LEFT WCs, providing a transparent connection between the underlying flavor structures and the observable nucleon decay rates [25, 48]:

$$\begin{aligned} \Gamma(p \rightarrow K^+ \nu_r) &= \frac{(m_p^2 - m_K^2)^2}{32\pi f_\pi^2 m_p^3} \left| \alpha[L_{dud}^{S,RL}]_{112r} - \beta[L_{udd}^{S,LL}]_{112r} + \frac{m_p}{2m_\Sigma} (D - F) (\alpha[L_{dud}^{S,RL}]_{211r} - \beta[L_{udd}^{S,LL}]_{121r}) \right. \\ &\quad \left. + \frac{m_p}{6m_\Lambda} (D + 3F) (\alpha[L_{dud}^{S,RL}]_{211r} - \beta[L_{udd}^{S,LL}]_{121r} + 2\alpha[L_{dud}^{S,RL}]_{112r} - 2\beta[L_{udd}^{S,LL}]_{112r}) \right|^2, \\ \Gamma(p \rightarrow \pi^0 \ell_r^+) &= \frac{(m_p^2 - m_\pi^2)^2}{32\pi f_\pi^2 m_p^3} \frac{(1 + D + F)^2}{2} \left\{ \left| \alpha[L_{duu}^{S,RL}]_{111r} + \beta[L_{duu}^{S,LL}]_{111r} \right|^2 + \left| \alpha[L_{duu}^{S,LR}]_{111r} + \beta[L_{duu}^{S,RR}]_{111r} \right|^2 \right\}, \\ \Gamma(p \rightarrow K^0 \ell_r^+) &= \frac{(m_p^2 - m_K^2)^2}{32\pi f_\pi^2 m_p^3} \left\{ \left| \beta[L_{duu}^{S,LL}]_{211r} - \alpha[L_{duu}^{S,RL}]_{211r} + \frac{m_p}{m_\Sigma} (D - F) (\beta[L_{duu}^{S,LL}]_{211r} + \alpha[L_{duu}^{S,RL}]_{211r}) \right|^2 \right. \\ &\quad \left. + \left| \beta[L_{duu}^{S,RR}]_{211r} - \alpha[L_{duu}^{S,LR}]_{211r} + \frac{m_p}{m_\Sigma} (D - F) (\beta[L_{duu}^{S,RR}]_{211r} + \alpha[L_{duu}^{S,LR}]_{211r}) \right|^2 \right\}. \end{aligned} \quad (24)$$

³ Alternatively, Refs. [52, 53] determine proton-decay matrix elements directly from lattice QCD, bypassing $B\chi$ PT.

In Eq. (24), m_X denotes the mass of the hadron or meson, and $f_\pi = 139$ MeV is the pion decay constant. The parameters α and β are real low-energy constants that parameterize the two independent nu-

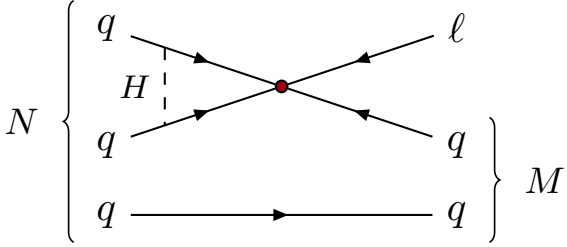


FIG. 1. Representative one-loop diagram contributing to two-body proton decay, $N \rightarrow M\ell$, where N denotes a nucleon decaying into a pseudoscalar meson M and a lepton ℓ . The red blob indicates a BNV vertex involving fermions of heavier generations, generated via the spurion expansion of a generic dimension-six BNV operator. The dashed line corresponds to the exchange of a SM Higgs boson, which mediates the flavor-changing transition to light-generation fermions.

cleon matrix elements arising from the three-quark operators. Their numerical values, extracted from lattice QCD, are taken as $\alpha = -0.01257(11)$ GeV³ and $\beta = 0.01269(107)$ GeV³ [52, 53]. The coefficients D and F denote the axial couplings of the baryon octet, which appear in the $B\chi$ PT Lagrangian. These constants can be obtained either phenomenologically, with $D = 0.80(1)$ and $F = 0.47(1)$ [54], or from lattice computations, which yield $D = 0.730(11)$ and $F = 0.447^{(6)}_{(7)}$ [55]. Also note that for neutrino final states, the decay width implicitly sums over the three neutrino flavors ($r = e, \mu, \tau$), which are experimentally indistinguishable.

As an important complementary step to the matching framework outlined above, our analysis incorporates the full renormalization-group (RG) evolution of the BNV operators down to hadronic scales. This evolution is carried out using `DsixTools` [56, 57], which includes the one-loop anomalous dimensions of the BNV operators [45] and consistently implements the SMEFT-LEFT matching conditions. Radiative effects play a crucial role, as operator mixing at one loop generates the LEFT structures that mediate proton decay even when absent at tree level; a representative contribution is displayed in Fig. 1. In cases where two-loop effects are required to connect high-scale operators to low-energy observables, sequential one-loop running provides an efficient approximation, evolving the coefficients down to the 2 GeV scale relevant for hadronic matrix elements. As highlighted in Ref. [32], these contributions scale as $\left(\frac{1}{16\pi^2} \log \frac{\Lambda^2}{m_{\text{EW}}^2}\right)^2$.

2. Results

The main results of the numerical analysis are summarized in Tab. 3. The corresponding bounds are expressed in terms of the effective ratio $\mathcal{R}_{\text{BL}} = \Lambda_{\text{B}}^2/\Lambda_{\text{L}}$, which connects the two UV scales. All results in Tab. 3 are quoted for the NO spectrum. At the precision relevant for this analysis, the bounds on the ratio \mathcal{R}_{BL} in the IO case can

be obtained by applying the inverse of the rescaling associated with the leptonic flavor invariants in NO and IO, as given in Eqs. (A12) and (A13) of App. A. Consequently, for operators involving \mathcal{T}_ℓ (\mathcal{T}_e), the IO bound on \mathcal{R}_{BL} is scaled by a factor of 0.8 (1.7) relative to the NO one. For each operator we report the strongest bound obtained in both the up and down flavor bases, corresponding to the most constraining decay channel in each case.

Additionally, the overall impact of the extended MFV framework on the allowed BNV parameter space in the context of present and future experiments is illustrated in Fig. 2. For each of the four dimension-six BNV operators, we use the leading spurion structures identified above and compute the proton lifetime τ_p as a function of the BNV scale Λ_{B} , while fixing Λ_{L} to several benchmark values displayed in the figure obeying the consistency relation $\Lambda_{\text{B}} \leq \Lambda_{\text{L}}$. The diagonal bands show the predicted lifetimes for fixed values of Λ_{L} , while the horizontal lines indicate the current limits from Super-K and the projected sensitivities of Hyper-K [21] for the $p \rightarrow \pi^0\ell^+$ channel and of DUNE [22] for the $p \rightarrow K^+\nu$ mode. The intersections of these curves determine the minimal values of Λ_{B} compatible with a given choice of Λ_{L} .

These results reveal a substantial spread in the BNV scales associated with different operators. For three of the four operators, in particular \mathcal{O}_{duql} , \mathcal{O}_{qque} , and \mathcal{O}_{duue} , whose leading contribution to proton decay is induced radiatively at one-loop level (see the following subsection for details), proton-decay limits are compatible with BNV scales in the multi-TeV range, provided the LNV scale Λ_{L} lies around $\mathcal{O}(10^3 \text{ TeV})$, $\mathcal{O}(10^6 \text{ TeV})$, and $\mathcal{O}(10^9 \text{ TeV})$, respectively. In contrast, \mathcal{O}_{qqgl} remains exceptionally constrained, requiring $\Lambda_{\text{B}} \gtrsim 10^7 \text{ TeV}$. Although the values of Λ_{L} inferred in this way are considerably lower than the naive expectation $\Lambda_{\text{L}} \sim \mathcal{O}(10^{12} \text{ TeV})$ suggested by a minimal type-I seesaw origin of Υ_ν [3, 7], such hierarchies arise naturally in alternative neutrino-mass constructions. Examples include type-II seesaw models [58, 59] and inverse-seesaw scenarios [60], where the smallness of neutrino masses is governed by a technically natural source of LNV [61], allowing the corresponding scale to be significantly lower than the naive expectation without introducing substantial fine-tuning.

Lastly, to further quantify the impact of the different flavor structures listed in Tab. 3, it is instructive to examine the dominant decay widths associated with the *golden channels* $p \rightarrow \pi^0\ell_r^+$ and $p \rightarrow K^+\nu$, whose lifetime limits are expected to improve about an order of magnitude in upcoming experiments [21, 22]. A convenient way to display their relative importance is through the predicted ratio

$$r_\ell \equiv \frac{\Gamma(p \rightarrow \pi^0\ell^+)}{\Gamma(p \rightarrow K^+\nu)}, \quad \ell \in \{e, \mu\}, \quad (25)$$

expressed as a function of Λ_{B} . This ratio renders the renormalization-group dependence particularly transparent and eliminates the explicit dependence on Λ_{L} . In con-

Operator	Spurion expansion	\mathcal{R}_{BL}^{up} [TeV]	Channel	\mathcal{R}_{BL}^{down} [TeV]	Channel
$[\mathcal{O}_{qqq\ell}]^{prst}$	$\frac{1}{\Lambda_B^2} \varepsilon_{prs} [\mathcal{T}_\ell]_t$ $\frac{1}{\Lambda_B^2} \{ \varepsilon_{prx} [Y_u Y_u^\dagger]_s^x + \varepsilon_{pxs} [Y_u Y_u^\dagger]_r^x + \varepsilon_{xrs} [Y_u Y_u^\dagger]_p^x \} [\mathcal{T}_\ell]_t$	1×10^7 1×10^7	$p \rightarrow K^+ \nu$ $p \rightarrow K^+ \nu$	1×10^7 1×10^7	$p \rightarrow K^+ \nu$ $p \rightarrow K^+ \nu$
$[\mathcal{O}_{duq\ell}]^{prst}$	$\frac{1}{\Lambda_B^2} \varepsilon_{abs} [Y_u]_r^a [Y_d]_p^b [\mathcal{T}_\ell]_t$	2×10^{-1}	$p \rightarrow \pi^0 e^+$	2×10^{-1}	$p \rightarrow \pi^0 e^+$
$[\mathcal{O}_{qque}]^{prst}$	$\frac{1}{2\Lambda_B^2} \{ \varepsilon_{abp} [Y_u Y_u^\dagger]_r^b + \varepsilon_{abr} [Y_u Y_u^\dagger]_p^b \} [Y_u]_s^a [\mathcal{T}_e]_t$	2×10^{-4}	$p \rightarrow \pi^0 \mu^+$	3×10^{-2}	$p \rightarrow \pi^0 \mu^+$
$[\mathcal{O}_{duee}]^{prst}$	$\frac{1}{\Lambda_B^2} \varepsilon_{ars} [Y_u^\dagger Y_d]_p^a [\mathcal{T}_e]_t$	2×10^{-7}	$p \rightarrow \pi^0 \mu^+$	7×10^{-6}	$p \rightarrow K^0 \mu^+$

TABLE 3. Summary of the leading proton-decay constraints for the dimension-six BNV operators and their minimally spurion-suppressed flavor completions under the extended MFV hypothesis. The first column lists the effective operators, while the second displays the corresponding spurion expansion. The third (fifth) column reports the bounds on the ratio $\mathcal{R}_{BL} \equiv \Lambda_B^2/\Lambda_L$ in the up (down) basis, denoted as \mathcal{R}_{BL}^{up} (\mathcal{R}_{BL}^{down}), while the adjacent columns indicate the decay channel that provides the most stringent limit in each case. We note that the RG effects between Λ_B and m_p induce a mild logarithmic dependence, which slightly affects the bound on \mathcal{R}_{BL} . For $\mathcal{O}_{duq\ell}$ (up basis), the $p \rightarrow \pi^0 \mu^+$ limit is accompanied by $p \rightarrow K^+ \nu$, as shown in Fig. 3. For \mathcal{O}_{qque} (down basis), the constraint from $p \rightarrow \pi^0 \mu^+$ is accompanied by $p \rightarrow K^0 \mu^+$, which exhibits comparable sensitivity. Limits quoted in the table are obtained using Υ_ν evaluated for the NO spectrum.

trast, the projections shown in Fig. 2 necessarily depend on the choice of Λ_L in order to quantify experimental sensitivities. Fig. 3 shows the ratio r_ℓ for the leading spurion structures of $\mathcal{O}_{duq\ell}$, \mathcal{O}_{duee} , and \mathcal{O}_{qque} . We omit $\mathcal{O}_{qqq\ell}$, whose ratio is strongly suppressed ($\sim 10^{-4}$) owing to the fact that the neutrino mode is generated at tree level, whereas the charged-lepton channel is generated only radiatively. As discussed in Sec. III A, constructing MFV flavor invariants for the BNV operators necessarily involves inserting the leptonic triplet spurions \mathcal{T}_e or \mathcal{T}_ℓ . Numerically, the dominant entry of \mathcal{T}_ℓ is always the component associated with e or ν_e , whereas for \mathcal{T}_e the second component provides the leading contribution for both NO and IO (see App. A). Consequently, operators built with \mathcal{T}_e predominantly yield muonic final states. For this reason, in Fig. 3 we take $\ell = \mu$ for \mathcal{O}_{duee} and \mathcal{O}_{qque} , while for $\mathcal{O}_{duq\ell}$ we set $\ell = e$. Within this MFV framework, observing a proton-decay mode with a μ^+ in the final state, rather than an e^+ or a neutrino, would naturally single out \mathcal{O}_{duee} or \mathcal{O}_{qque} as the underlying operators. Conversely, if BNV were mainly induced by $\mathcal{O}_{duq\ell}$ with Λ_B near the multi-TeV regime, one would anticipate similar decay rates for $p \rightarrow \pi^0 e^+$ and $p \rightarrow K^+ \nu$.

3. Operator-by-Operator Discussion

In what follows, we briefly discuss the phenomenological implications of the individual BNV operators and the features of their dominant flavor structures.

$\mathcal{O}_{qqq\ell}$. Within the spurion counting, the leading flavor structures are $\mathcal{O}(Y_e^2 \Upsilon_\nu)$ and, at the next-to-leading order, $\mathcal{O}(Y_u^2 Y_e^2 \Upsilon_\nu)$. Although the latter carries an extra Y_u^2 insertion, the dominance of the top Yukawa ($y_t \simeq 1$) renders the numerical suppression modest, so both contributions are of comparable size. These structures contribute already at tree level to the proton decay, with the

most constraining channel being $p \rightarrow K^+ \nu_r$. Since the $\mathcal{O}(Y_e^2 \Upsilon_\nu)$ invariant does not involve quark-Yukawa insertions at the SMEFT level, no distinction between the up and down bases emerges until the subsequent matching onto the LEFT. Nonetheless, the resulting LEFT Wilson coefficients turn out to be identical in the two bases. In the up basis these coefficients can be expressed as

$$[L_{udd}^{S,LL}]_{112r} = -[L_{udd}^{S,LL}]_{121r} = \frac{3[\mathcal{T}_\ell]_r}{\Lambda_B^2} (V_{td} V_{cs} - V_{ts} V_{cd}), \quad (26)$$

whereas in the down basis they are given by

$$[L_{udd}^{S,LL}]_{112r} = -[L_{udd}^{S,LL}]_{121r} = -\frac{3[\mathcal{T}_\ell]_r}{\Lambda_B^2} V_{ub}^*. \quad (27)$$

This equality follows from a general identity for $n \times n$ matrices. For any matrix \mathbf{V} , the adjugate satisfies $\mathbf{V} \text{adj}(\mathbf{V}) = \det(\mathbf{V}) \mathbf{I}$. When \mathbf{V} is unitary, this reduces to $\text{adj}(\mathbf{V}) = \mathbf{V}^\dagger$. Evaluating the (1,3) component then yields the relation

$$V_{ts} V_{cd} - V_{td} V_{cs} = V_{ub}^*, \quad (28)$$

which precisely equates the CKM combinations appearing in the two expressions above.

For the $\mathcal{O}(Y_u^2 Y_e^2 \Upsilon_\nu)$ structure, the SMEFT invariant is already basis dependent: in the up basis one obtains a contraction proportional to $\sim \varepsilon_{pr3} y_t^2 \delta_{s3}$, whereas in the down basis the same structure transforms as $\sim \varepsilon_{prx} y_t^2 V_{tx}^* V_{ts}$. Analogously to the $\mathcal{O}(Y_e^2 \Upsilon_\nu)$ invariant, the LEFT coefficients entering $p \rightarrow K^+ \nu_r$ in the up basis are given by

$$[L_{udd}^{S,LL}]_{112r} = -[L_{udd}^{S,LL}]_{121r} = \frac{3y_t^2[\mathcal{T}_\ell]_r}{\Lambda_B^2} (V_{td} V_{cs} - V_{ts} V_{cd}), \quad (29)$$

while in the down basis the corresponding expression is obtained by the substitutions $V_{ts} V_{cd} - V_{td} V_{cs} \rightarrow V_{ub}^*$ and

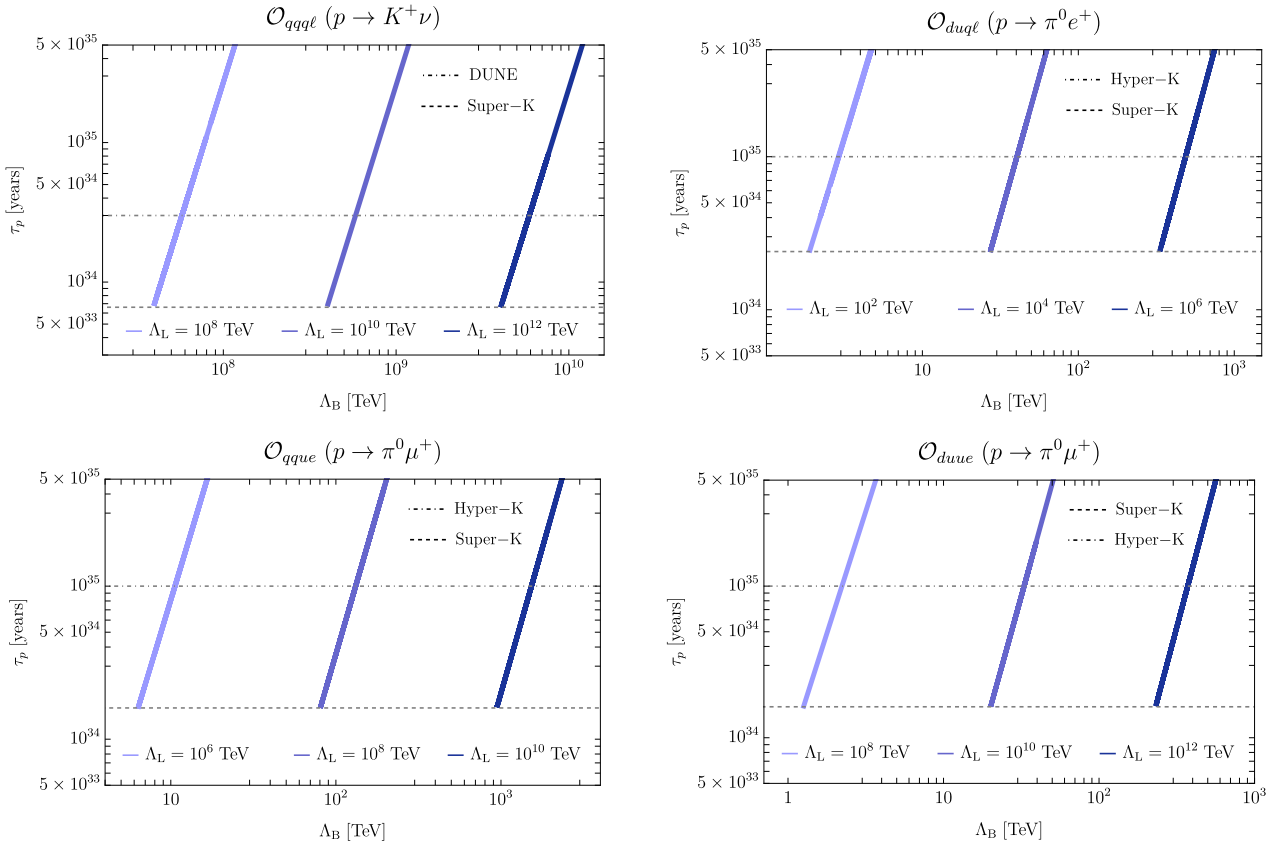


FIG. 2. Predicted proton lifetimes τ_p from the leading spurion expansion of baryon-number violating operators $\mathcal{O}_{qqq\ell}$, $\mathcal{O}_{duq\ell}$, \mathcal{O}_{qque} , and \mathcal{O}_{duue} from Tab. 1. The dashed and dot-dashed curves represent current (Super-K) and projected (Hyper-K, DUNE) experimental sensitivities, respectively. For each operator, we vary Λ_L across three benchmark values to map the allowed Λ_B parameter space. The limiting decay channel for each case follows Tab. 3, with all lifetimes computed in the up-quark basis for concreteness.

$y_t^2 \rightarrow y_t^2 |V_{tb}|^2$. Given that $y_t, V_{tb} \simeq 1$, these modifications leave the overall magnitude essentially unchanged. The resulting LEFT coefficients are therefore of the same order as those generated by the $\mathcal{O}(Y_e^2 \Upsilon_\nu)$ structure, implying comparable sensitivities in the corresponding decay channels (see Tab. 3). In the full numerical analysis, we incorporate the RG evolution between the baryon-violating scale Λ_B and the hadronic scale $\mu \simeq 2$ GeV, as implemented in `DsixTools`. At tree level, the effective ratio $\mathcal{R}_{BL}^{\text{up}} \equiv \Lambda_B^2 / \Lambda_L$ is approximately 6×10^6 TeV, whereas the RG effects increase this value by a factor of ~ 2 , a typical enhancement for BNV operators whose anomalous dimensions are dominated by self-running [25].

$\mathcal{O}_{duq\ell}$. The dominant spurion structure for this operator, arising at $\mathcal{O}(Y_u Y_d Y_e^2 \Upsilon_\nu)$, already induces BNV at tree level, giving rise to the $p \rightarrow K^+ \nu_r$ channel, with the corresponding tree-level LEFT WCs evaluated in the up alignment as

$$\begin{aligned} [L_{dud}^{S,RL}]_{112r} &= -\frac{2m_u m_d}{v^2 \Lambda_B^2} [\mathcal{T}_\ell]_r (V_{ts} V_{cd} - V_{cs} V_{td}) , \\ [L_{dud}^{S,RL}]_{211r} &= -\frac{2m_u m_s}{v^2 \Lambda_B^2} [\mathcal{T}_\ell]_r (V_{td} V_{cs} - V_{ts} V_{cd}) . \end{aligned} \quad (30)$$

These coefficients remain non-vanishing in either flavor basis, as the CKM factors enter directly through the SMEFT-LEFT matching (see Tab. 2 and Eq. (23)). In addition to the neutrino channel, this operator also generates a charged-lepton mode $p \rightarrow K^0 \ell_r^+$, which arises at tree level only in the down alignment:

$$[L_{duu}^{S,RL}]_{211r} = -\frac{2m_u m_s}{v^2 \Lambda_B^2} V_{ub}^* [\mathcal{T}_\ell]_r , \quad (31)$$

while in the up alignment the corresponding coefficient vanishes due to the contraction of the form $\varepsilon_{ab1} [\widehat{Y}_u]^a_1 [V \widehat{Y}_d]^b_2$. In contrast, the tree-level amplitude for $p \rightarrow \pi^0 \ell_r^+$ vanishes in both flavor bases. However, from a phenomenological standpoint, this mode provides the strongest experimental sensitivity among all two-body decay channels. Although absent at tree level, RG evolution radiatively induces the corresponding effective operators, and the resulting contributions ultimately set the most stringent bounds on this class of interactions. As an explicit example, following the SMEFT-LEFT matching in the up-aligned basis, the non-vanishing coefficients relevant for the $p \rightarrow \pi^0 \ell_r^+$ transition in the

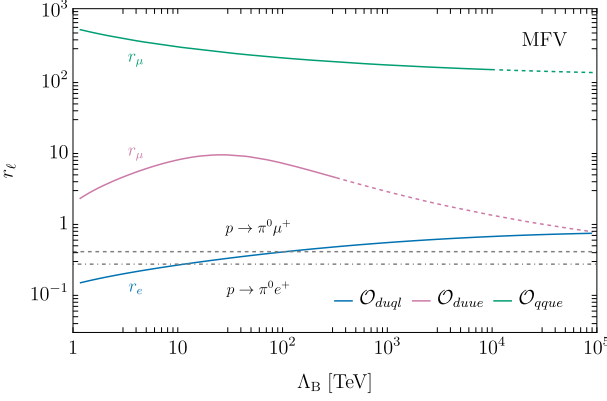


FIG. 3. Ratio of the proton-decay channels $p \rightarrow \pi^0 \ell^+$ and $p \rightarrow K^+ \nu$ defined in Eq. (25) as a function of Λ_B for the three spurion expansions relevant in the MFV framework (see Tab. 1). The predictions for \mathcal{O}_{duu} and \mathcal{O}_{qque} correspond to the muonic channel, while those for \mathcal{O}_{duql} correspond to the electron mode $p \rightarrow \pi^0 e^+$. The horizontal dashed (dot-dashed) gray lines indicate the experimental values from Super-K for the electronic (muonic) channel; operator curves lying above (below) these lines are therefore more tightly constrained by $p \rightarrow \pi^0 \ell^+$ ($p \rightarrow K^+ \nu$), in agreement with Tab. 3. For \mathcal{O}_{duu} and \mathcal{O}_{qque} , solid (dashed) segments denote the regions where Λ_L is below (above) 10^{12} TeV, with the latter being the maximal scale compatible with a weakly-coupled regime of a UV seesaw origin of Υ_ν . The dashed portions remain phenomenologically viable, but observable proton decay in this regime would require $\Lambda_L > 10^{12}$ TeV. All decay widths are computed in the up-quark basis; see the main text for details.

leading-log approximation can be written as

$$\begin{aligned} [L_{duu}^{S,RL}]_{111r} &\simeq \frac{m_u m_d m_s m_b}{4\pi^2 v^4 \Lambda_B^2} [\mathcal{T}_\ell]_r V_{tb} V_{td} V_{us}^* \log \frac{\mu_f}{\Lambda_B}, \\ [L_{duu}^{S,LL}]_{111r} &\simeq -\frac{m_d m_s m_t^2}{2\pi^2 v^4 \Lambda_B^2} [\mathcal{T}_\ell]_r V_{cd} V_{cs} V_{td} \log \frac{\mu_f}{\Lambda_B}, \\ [L_{duu}^{S,LR}]_{111r} &\simeq \frac{m_u m_d m_b m_{\ell_r}}{4\pi^2 v^4 \Lambda_B^2} [\mathcal{T}_\ell]_r V_{cd} V_{tb} V_{td} \log \frac{\mu_f}{\Lambda_B}, \end{aligned} \quad (32)$$

where μ_f denotes the renormalization scale at which the SMEFT is matched onto the LEFT, typically taken to be of $\mathcal{O}(\mu_{EW})$.

\mathcal{O}_{qque} . The leading spurion structure associated with this operator, which is of $\mathcal{O}(Y_u^3 Y_e^3 \Upsilon_\nu)$, involves solely the insertions of up-type Yukawa matrices. Consequently, its phenomenological impact depends explicitly on the choice of flavor basis, exhibiting distinct structures in the up and down alignments. Starting with the down basis, where essentially all flavor components of the operator remain non-vanishing, BNV transition occurs already at tree level. The dominant contribution arises through the $p \rightarrow \pi^0 \ell^+$ channel, with the leading LEFT WC given by

$$[L_{duu}^{S,LR}]_{111r} = -\frac{4\sqrt{2} m_t^2 m_c}{v^3 \Lambda_B^2} V_{td} V_{cs}^* V_{tb}^* V_{ud}^* V_{us}^* [\mathcal{T}_e]_r. \quad (33)$$

Given that the components of the leptonic spurion satisfy $|\mathcal{T}_e|_2/|\mathcal{T}_e|_1|_{NO(10)} \simeq 70(40)$ (see App. A), the current Super-K limits, whose sensitivities are comparable for final-state e^+ and μ^+ , imply that the $p \rightarrow \pi^0 \mu^+$ channel provides the strongest constraint among the corresponding decay modes [18].

Conversely, in the up basis, only a limited subset of SMEFT WCs remain non-vanishing at the high scale:

$$\begin{aligned} [\mathcal{C}_{qque}]_{123r} &= [\mathcal{C}_{qque}]_{213r} = -\frac{\sqrt{2} m_t (m_c^2 - m_u^2)}{v^3 \Lambda_B^2} [\mathcal{T}_e]_r, \\ [\mathcal{C}_{qque}]_{132r} &= [\mathcal{C}_{qque}]_{312r} = \frac{\sqrt{2} m_c (m_t^2 - m_u^2)}{v^3 \Lambda_B^2} [\mathcal{T}_e]_r, \\ [\mathcal{C}_{qque}]_{321r} &= [\mathcal{C}_{qque}]_{231r} = -\frac{\sqrt{2} m_u (m_t^2 - m_c^2)}{v^3 \Lambda_B^2} [\mathcal{T}_e]_r. \end{aligned} \quad (34)$$

Upon SMEFT-LEFT matching, no tree-level LEFT operators mediating two-body proton decay are induced. In the up basis, BNV therefore emerges only via operator mixing, leading to a weaker constraint on \mathcal{R}_{BL}^{up} , as shown in Tab. 3. In particular, in the leading-log approximation, the only non-vanishing LEFT coefficient contributing to the $p \rightarrow \pi^0 \ell^+$ channel is given by

$$[L_{duu}^{S,LR}]_{111r} \simeq \frac{m_u m_d m_b m_t^2}{4\sqrt{2} \pi v^5 \Lambda_B^2} [\mathcal{T}_e]_r V_{cd}^2 V_{cb}^* \log \frac{\mu_f}{\Lambda_B}. \quad (35)$$

In conclusion, the $p \rightarrow \pi^0 \mu^+$ channel remains the dominant probe in either basis. The additional Y_e factor encoded in \mathcal{T}_e imposes an extra parametric suppression on the relevant LEFT coefficient, resulting in a comparatively weaker bound.

\mathcal{O}_{duu} . The lowest-order spurion structure associated with this operator appears at $\mathcal{O}(Y_u Y_d Y_e^2 \Upsilon_\nu)$. An important feature of this combination is that its basis dependence is significantly reduced compared to the spurion structures arising in the other dimension-six BNV operators: the factor $Y_u^\dagger Y_d$ transforms covariantly under flavor rotations and, upon switching between the up- and down-aligned bases, it is simply rewritten as $Y_u^\dagger Y_d \rightarrow \hat{Y}_u^\dagger V \hat{Y}_d$. As a result, the overall spurion structure extracted from this operator is effectively the same in both bases.

At the level of the low-energy theory, \mathcal{O}_{duu} matches onto the $\mathcal{O}_{duu}^{S,RR}$ scalar operator (see Tab. 2), which contributes to the $p \rightarrow \pi^0 \ell^+$ and $p \rightarrow K^+ \ell^+$ channels. However, due to the antisymmetric ε -tensor contraction in the SMEFT operator, all tree-level LEFT coefficients leading to two-body proton decay vanish, independently of the chosen flavor basis.⁴ Consequently, any phenomenologi-

⁴ In configurations involving higher-generation right-handed up-type quarks [29] or bottom quarks [30] the heavy quark appears off shell and hadronizes into multi-body final states, giving rise to proton-decay channels that are phase-space suppressed and experimentally subleading. An analogous suppression arises for operators involving tau leptons [31, 33, 35].

Field	Type	UV Lagrangian	BNV Operators generated
ω_1 (3, 1)_{-1/3}	S	$[y_{\omega_1}^{q\ell}]^s_{pr} \omega_{1s}^\dagger \bar{q}^c p i \sigma_2 \ell^r + [y_{\omega_1}^{qq}]^{spr} \omega_{1s}^{\alpha\dagger} \varepsilon_{\alpha\beta\gamma} \bar{q}_p^\beta i \sigma_2 q_r^{c\gamma} + [y_{\omega_1}^{eu}]^s_{pr} \omega_{1s}^\dagger \bar{e}^c p u^r + [y_{\omega_1}^{du}]^{spr} \omega_{1s}^{\alpha\dagger} \varepsilon_{\alpha\beta\gamma} \bar{d}_p^\beta u_r^{c\gamma} + \text{h.c.}$	$\mathcal{O}_{duq\ell}, \mathcal{O}_{qque}, \mathcal{O}_{qqql}, \mathcal{O}_{duue}$
ω_4 (3, 1)_{-4/3}	S	$[y_{\omega_4}^{qd}]^s_{pr} \omega_{4s}^\dagger \bar{e}^c p d^r + [y_{\omega_4}^{uu}]^{spr} \omega_{4s}^{\alpha\dagger} \varepsilon_{\alpha\beta\gamma} \bar{u}_p^\beta u_r^{c\gamma} + \text{h.c.}$	\mathcal{O}_{duue}
ζ (3, 3)_{-1/3}	S	$[y_\zeta^{q\ell}]^s_{pr} \zeta_s^A \bar{q}^c p i \sigma_2 \sigma^A \ell^r + [y_\zeta^{qq}]^{spr} \zeta_s^{\alpha\dagger} \varepsilon_{\alpha\beta\gamma} \bar{q}_p^\beta \sigma^A i \sigma_2 q_r^{c\gamma} + \text{h.c.}$	\mathcal{O}_{qqql}
\mathcal{Q}_1 (3, 2)_{1/6}	V	$[g_{\mathcal{Q}_1}^{u\ell}]^s_{pr} \mathcal{Q}_{1s}^{\mu\dagger} \bar{u}^c p \gamma_\mu \ell^r + [g_{\mathcal{Q}_1}^{uq}]^{spr} \mathcal{Q}_{1s}^{\mu\alpha\dagger} \varepsilon_{\alpha\beta\gamma} \bar{d}_p^\beta \gamma_\mu i \sigma_2 q_r^{c\gamma} + \text{h.c.}$	\mathcal{O}_{duql}
\mathcal{Q}_5 (3, 2)_{-5/6}	V	$[g_{\mathcal{Q}_5}^{d\ell}]^s_{pr} \mathcal{Q}_{5s}^{\mu\dagger} \bar{d}^c p \gamma_\mu \ell^r + [g_{\mathcal{Q}_5}^{eq}]^{spr} \mathcal{Q}_{5s}^{\mu\alpha\dagger} \varepsilon_{\alpha\beta\gamma} \bar{u}_p^\beta \gamma_\mu q_r^{c\gamma} + \text{h.c.}$	$\mathcal{O}_{duql}, \mathcal{O}_{qque}$

TABLE 4. Overview of the leptoquark (LQ) mediators considered in our UV analysis, using the notation of Ref. [62]. The first column lists the mediators and their transformation properties under the SM gauge group. The second column indicates whether the given LQ gauge irrep is a scalar (S) or vector (V) field. The third column presents the allowed renormalizable interaction terms involving the LQs and SM fermions, written without imposing any flavor symmetry assumptions. The final column lists the BNV operators that result from integrating out the corresponding LQ mediator at tree level. As in Tab. 1, Greek indices α, β, γ label $SU(3)_C$, while p, r, s represent flavor indices, with p, r for fermions and s for the mediator. In case of ζ mediator, A denotes the $SU(2)_L$ adjoint index, whereas the remaining $SU(2)_L$ contractions are left implicit. For couplings involving identical fermion fields, the associated flavor tensors are subject to additional symmetry relations, which constrain the number of independent flavor structures. In particular, $[y_{\omega_1}^{qq}]^{spr}$ flavor tensor is symmetric, whereas $[y_{\omega_4}^{uu}]^{spr}$ and $[y_\zeta^{qq}]^{spr}$ are antisymmetric under the exchange of quark indices $p \leftrightarrow r$.

cal impact of this operator arises only radiatively through operator mixing.

In the leading-log approximation, the radiatively generated LEFT coefficients relevant for the two dominant decay channels take different forms depending on the flavor alignment. In particular, in the up-aligned basis, the non-vanishing contributions are

$$\begin{aligned} [L_{duu}^{S,LR}]_{111r} &\simeq -\frac{m_d m_c m_b m_t}{4\pi^2 v^4 \Lambda_B^2} [\mathcal{T}_e]_r V_{cd} V_{tb} V_{td} \log \frac{\mu_f}{\Lambda_B}, \\ [L_{duu}^{S,LR}]_{211r} &\simeq -\frac{m_d m_c m_b m_t}{4\pi^2 v^4 \Lambda_B^2} [\mathcal{T}_e]_r V_{cs} V_{tb} V_{td} \log \frac{\mu_f}{\Lambda_B}, \end{aligned} \quad (36)$$

while in the down basis the corresponding expressions read

$$\begin{aligned} [L_{duu}^{S,LR}]_{111r} &\simeq -\frac{m_u m_t m_b^2}{4\pi^2 v^4 \Lambda_B^2} [\mathcal{T}_e]_r V_{tb} V_{td} V_{us}^* \log \frac{\mu_f}{\Lambda_B}, \\ [L_{duu}^{S,LR}]_{211r} &\simeq -\frac{m_u m_t m_b^2}{4\pi^2 v^4 \Lambda_B^2} [\mathcal{T}_e]_r V_{tb} V_{ts} V_{us}^* \log \frac{\mu_f}{\Lambda_B}. \end{aligned} \quad (37)$$

Additionally, in the down basis, operator mixing also induces $L_{duu}^{S,RL}$ structures, suppressed by the charged-lepton mass

$$\begin{aligned} [L_{duu}^{S,RL}]_{111r} &\simeq \frac{m_u m_d m_t m_{\ell_r}}{4\pi^2 v^4 \Lambda_B^2} [\mathcal{T}_e]_r V_{td} V_{us}^* \log \frac{\mu_f}{\Lambda_B}, \\ [L_{duu}^{S,RL}]_{211r} &\simeq \frac{m_u m_s m_t m_{\ell_r}}{4\pi^2 v^4 \Lambda_B^2} [\mathcal{T}_e]_r V_{ts} V_{us}^* \log \frac{\mu_f}{\Lambda_B}. \end{aligned} \quad (38)$$

Evaluating the relevant LEFT coefficients using the full RG evolution implemented in `DsixTools`, one finds that the resulting limits are driven by the $p \rightarrow \pi^0 \mu^+$ and $p \rightarrow K^0 \mu^+$ modes. As summarized in Tab. 3, these two channels ultimately provide comparable sensitivity. In addition, as shown in the rightmost panel of Fig. 3, for sufficiently large Λ_B the RG evolution can alter which proton-decay mode provides the leading constraint. In particular, for $\Lambda_B \gtrsim 3 \times 10^4$ TeV, the $p \rightarrow K^+ \nu$ decay channel becomes dominant over $p \rightarrow \pi^0 \mu^+$, yet proton-decay rates near current sensitivities would nevertheless

require Λ_L to lie close to the Planck scale, rendering the scenario phenomenologically nonviable.

IV. BNV BEYOND THE EFT DESCRIPTION

The preceding section presented a systematic study of the flavor structures associated with the dimension-six BNV operators and their impact on proton-decay phenomenology. Following this analysis, we now turn to the question of their UV origin. Our aim is to identify the tree-level UV completions capable of generating the BNV operators analyzed in Sec. III, while at the same time going beyond the leading-order EFT treatment.⁵

In particular, this section focuses on single-mediator extensions of the SM. Tree-level generation of a dimension-six BNV operator uniquely points to leptoquarks (LQs) as the only viable mediator types [62, 65]. The five relevant LQ representations, along with their renormalizable couplings and the BNV operators they generate at tree level, are summarized in Tab. 4.

Based on the well-established practice of assigning non-trivial flavor charges to new-physics mediators in baryon-number-conserving (BNC) SMEFT [42, 43, 66, 67], we impose the extended MFV hypothesis at the UV level by allowing the LQ mediators to transform nontrivially under the flavor group. This procedure dictates the spurion transformation properties of the renormalizable UV couplings and enables a systematic classification of the LQ representations consistent with flavor-invariant interaction terms.

Tabs. 5 and 6 summarize the representative flavor assignments for the scalar and vector LQ mediators considered in this work, each capable of generating BNV

⁵ For loop-level completions of BNV SMEFT operators see Refs. [46, 63, 64].

ω_1 irreps	$y_{\omega_1}^{q\ell}$	$y_{\omega_1}^{qq}$	$\mathcal{O}_{qqq\ell}$	$\mathcal{O}_{duu\ell}$
$\mathbf{3}_q$	$\delta^s{}_p [\mathcal{T}_\ell]_r$	$\varepsilon^{sx(p)} [Y_u Y_u^\dagger]^{r)}_x$	$\mathcal{O}(Y_u^2 Y_e^2 \Upsilon_\nu)$	$\mathcal{O}(Y_u Y_d Y_e^2 \Upsilon_\nu)$
$\mathbf{3}_u$	$[Y_u^\dagger]_s {}^p [\mathcal{T}_\ell]_r$	$[Y_u^\dagger]_s {}^y \varepsilon^{yx(p)} [Y_u Y_u^\dagger]^{r)}_x$	$\mathcal{O}(Y_u^4 Y_e^2 \Upsilon_\nu)$	$\mathcal{O}(Y_u^2 Y_d Y_e^2 \Upsilon_\nu)$
$\overline{\mathbf{6}}_q$	$\varepsilon_{yp(s)} [Y_u Y_u^\dagger]^{y s)} [\mathcal{T}_\ell]_r$	$\delta^{(p)}_s \delta^{(r)}_{s'}$	$\mathcal{O}(Y_u^2 Y_e^2 \Upsilon_\nu)$	$\mathcal{O}(Y_u^3 Y_d Y_e^2 \Upsilon_\nu)$
$(\mathbf{3}_q, \mathbf{3}_\ell)$	$\delta^s{}_p (\delta^{s'}{}_r + [\Upsilon_\nu \Upsilon_\nu^\dagger]^{s'}{}_r)$	$[\mathcal{T}_\ell^\dagger]^{s'} \varepsilon^{sx(p)} [Y_u Y_u^\dagger]^{r)}_x$	$\mathcal{O}(Y_u^2 Y_e^2 \Upsilon_\nu)$	$\mathcal{O}(Y_u Y_d Y_e^2 \Upsilon_\nu)$
$(\mathbf{3}_u, \mathbf{3}_\ell)$	$[Y_u^\dagger]_s {}^p (\delta^{s'}{}_r + [\Upsilon_\nu \Upsilon_\nu^\dagger]^{s'}{}_r)$	$[\mathcal{T}_\ell^\dagger]^{s'} [Y_u^\dagger]_s {}^y \varepsilon^{yx(p)} [Y_u Y_u^\dagger]^{r)}_x$	$\mathcal{O}(Y_u^4 Y_e^2 \Upsilon_\nu)$	$\mathcal{O}(Y_u^2 Y_d Y_e^2 \Upsilon_\nu)$
$(\mathbf{3}_q, \overline{\mathbf{3}}_\ell)$	$\delta^s{}_p [\Upsilon_\nu^\dagger]_{s'} {}^r$	$[\mathcal{T}_\ell]_{s'} \varepsilon^{sx(p)} [Y_u Y_u^\dagger]^{r)}_x$	$\mathcal{O}(Y_u^2 Y_e^2 \Upsilon_\nu^2)$	$\mathcal{O}(Y_u Y_d Y_e^2 \Upsilon_\nu^2)$
ω_1 irreps	$y_{\omega_1}^{eu}$	$y_{\omega_1}^{du}$	$\mathcal{O}_{\ell q}^{(1,3)}$	\mathcal{O}_{eu}
$\mathbf{3}_q$	$[Y_u]_s {}^r [\mathcal{T}_e]_p$	$\varepsilon^{sxy} [Y_d^\dagger]_p {}^x [Y_u^\dagger]_y {}^r$	$\mathcal{O}(Y_e^4 \Upsilon_\nu^2)$	$\mathcal{O}(Y_u^2 Y_e^6 \Upsilon_\nu^2)$
$\mathbf{3}_u$	$\delta^s{}_r [\mathcal{T}_e]_p$	$\varepsilon^{srx} [Y_d^\dagger Y_u]_p {}^x$	$\mathcal{O}(Y_u^2 Y_e^4 \Upsilon_\nu^2)$	$\mathcal{O}(Y_e^6 \Upsilon_\nu^2)$
$\overline{\mathbf{6}}_q$	$\varepsilon_{yx(s)} [Y_u Y_u^\dagger]^{y s)} [Y_u]_x {}^r [\mathcal{T}_e]_p$	$[Y_d^\dagger]_p {}^s {}_x [Y_u^\dagger]_y {}^r$	$\mathcal{O}(Y_u^4 Y_e^4 \Upsilon_\nu^2)$	$\mathcal{O}(Y_u^6 Y_e^6 \Upsilon_\nu^2)$
$(\mathbf{3}_q, \mathbf{3}_\ell)$	$[Y_u]_s {}^r (\delta^{s'}{}_x + [\Upsilon_\nu \Upsilon_\nu^\dagger]^{s'}{}_x) [Y_e]_x {}^p$	$\varepsilon^{sxy} [Y_d^\dagger]_p {}^x [Y_u^\dagger]_y {}^r [\mathcal{T}_\ell^\dagger]^{s'}$	$\mathcal{O}(\Upsilon_\nu^2)$	$\mathcal{O}(Y_u^2 Y_e^2 \Upsilon_\nu^2)$
$(\mathbf{3}_u, \mathbf{3}_\ell)$	$\delta^s{}_r (\delta^{s'}{}_x + [\Upsilon_\nu \Upsilon_\nu^\dagger]^{s'}{}_x) [Y_e]_x {}^p$	$\varepsilon^{srx} [Y_d^\dagger Y_u]_p {}^x [\mathcal{T}_\ell^\dagger]^{s'}$	$\mathcal{O}(Y_u^2 \Upsilon_\nu^2)$	$\mathcal{O}(Y_e^2 \Upsilon_\nu^2)$
$(\mathbf{3}_q, \overline{\mathbf{3}}_\ell)$	$[Y_u]_s {}^r [\Upsilon_\nu^\dagger Y_e]_{s'} {}^p$	$\varepsilon^{sxy} [Y_d^\dagger]_p {}^x [Y_u^\dagger]_y {}^r [\mathcal{T}_\ell]_{s'}$	$\mathcal{O}(\Upsilon_\nu^2)$	$\mathcal{O}(Y_u^2 Y_e^2 \Upsilon_\nu^2)$
ω_4 irreps	$y_{\omega_4}^{ed}$	$y_{\omega_4}^{uu}$	\mathcal{O}_{duue}	\mathcal{O}_{ed}
$\mathbf{3}_q$	$[Y_d]_s {}^r [\mathcal{T}_e]_p$	$[Y_u]_s {}_x \varepsilon^{xpr}$	$\mathcal{O}(Y_u Y_d Y_e^3 \Upsilon_\nu)$	$\mathcal{O}(Y_d^2 Y_e^6 \Upsilon_\nu^2)$
$\mathbf{3}_d$	$\delta^s{}_r [\mathcal{T}_e]_p$	$[Y_d^\dagger Y_u]_s {}_x \varepsilon^{xpr}$	$\mathcal{O}(Y_u Y_d Y_e^3 \Upsilon_\nu)$	$\mathcal{O}(Y_e^6 \Upsilon_\nu^2)$
$(\mathbf{3}_q, \mathbf{3}_\ell)$	$[Y_d]_s {}^r (\delta^{s'}{}_y + [\Upsilon_\nu \Upsilon_\nu^\dagger]^{s'}{}_y) [Y_e]_y {}^p$	$[\mathcal{T}_\ell^\dagger]^{s'} [Y_u]_s {}_x \varepsilon^{xpr}$	$\mathcal{O}(Y_u Y_d Y_e^3 \Upsilon_\nu)$	$\mathcal{O}(Y_d^2 Y_e^2 \Upsilon_\nu^2)$
$(\mathbf{3}_d, \mathbf{3}_\ell)$	$\delta^s{}_r (\delta^{s'}{}_y + [\Upsilon_\nu \Upsilon_\nu^\dagger]^{s'}{}_y) [Y_e]_y {}^p$	$[\mathcal{T}_\ell^\dagger]^{s'} [Y_d^\dagger Y_u]_s {}_x \varepsilon^{xpr}$	$\mathcal{O}(Y_u Y_d Y_e^3 \Upsilon_\nu)$	$\mathcal{O}(Y_e^2 \Upsilon_\nu^2)$
$(\mathbf{3}_d, \overline{\mathbf{3}}_\ell)$	$\delta^s{}_r [\Upsilon_\nu^\dagger Y_e]_{s'} {}^p$	$[\mathcal{T}_\ell]_{s'} [Y_d^\dagger Y_u]_s {}_x \varepsilon^{xpr}$	$\mathcal{O}(Y_u Y_d Y_e^3 \Upsilon_\nu)$	$\mathcal{O}(Y_e^2 \Upsilon_\nu^2)$
ζ irreps	$y_\zeta^{q\ell}$	y_ζ^{qq}	$\mathcal{O}_{qqq\ell}$	$\mathcal{O}_{\ell q}^{(1,3)}$
$\mathbf{3}_q$	$\delta^s{}_p [\mathcal{T}_\ell]_r$	ε^{spr}	$\mathcal{O}(Y_e^2 \Upsilon_\nu)$	$\mathcal{O}(Y_e^4 \Upsilon_\nu^2)$
$\mathbf{3}_u$	$[Y_u^\dagger]_s {}^p [\mathcal{T}_\ell]_r$	$[Y_u^\dagger]_s {}_y \varepsilon^{ypr}$	$\mathcal{O}(Y_u^2 Y_e^2 \Upsilon_\nu)$	$\mathcal{O}(Y_u^2 Y_e^4 \Upsilon_\nu^2)$
$(\mathbf{3}_q, \mathbf{3}_\ell)$	$\delta^s{}_p (\delta^{s'}{}_r + [\Upsilon_\nu \Upsilon_\nu^\dagger]^{s'}{}_r)$	$[\mathcal{T}_\ell^\dagger]^{s'} \varepsilon^{spr}$	$\mathcal{O}(Y_e^2 \Upsilon_\nu)$	$\mathcal{O}(\Upsilon_\nu^2)$
$(\mathbf{3}_u, \mathbf{3}_\ell)$	$[Y_u^\dagger]_s {}^p (\delta^{s'}{}_r + [\Upsilon_\nu \Upsilon_\nu^\dagger]^{s'}{}_r)$	$[\mathcal{T}_\ell^\dagger]^{s'} [Y_u^\dagger]_s {}_y \varepsilon^{ypr}$	$\mathcal{O}(Y_u^2 Y_e^2 \Upsilon_\nu)$	$\mathcal{O}(Y_u^2 \Upsilon_\nu^2)$
$(\mathbf{3}_q, \overline{\mathbf{3}}_\ell)$	$\delta^s{}_p [\Upsilon_\nu^\dagger]_{s'} {}^r$	$[\mathcal{T}_\ell]_{s'} \varepsilon^{spr}$	$\mathcal{O}(Y_e^2 \Upsilon_\nu^2)$	$\mathcal{O}(\Upsilon_\nu^2)$

TABLE 5. Overview of the leading spurionic flavor invariants for the couplings of the scalar leptoquarks ω_1 , ω_4 , and ζ . The first column lists representative flavor irreducible representations (irreps) of each LQ. The second and third columns display the flavor structures of the allowed renormalizable couplings to SM fermions, expressed in terms of the relevant flavor spurions (see Tab. 4 for details). The final two columns report the characteristic spurionic suppression of the SMEFT Wilson coefficients induced at tree level, both for the BNV operators and for a representative baryon-number-conserving operator entering $\mu - e$ conversion. The flavor indices p and r label the SM fermions appearing in the coupling tensors (e.g. two quarks for $y_{\omega_1, \zeta}^{qq}$ or $y_{\omega_4}^{uu}$, and a quark-lepton pair for $y_{\omega_1, \zeta}^{q\ell}$ or $y_{\omega_4}^{ed}$). Each LQ field carries either a single flavor index s when transforming in a fundamental representation of G_F , or a pair of indices (s, s') when transforming as a sextet or bifundamental. We employ the notation $2\psi_{(a|\chi|b)} = \psi_a \chi_b + \psi_b \chi_a$ to denote symmetrization over the indices a and b .

SMEFT operators at tree level. Within the extended MFV framework, none of these mediators may transform as a flavor singlet, since the quark sector admits no spurion in the $\mathbf{3}_f$ representation of G_F with $f \in \{q, u, d\}$, unlike the lepton sector, where such structures can be constructed (see App. A). Consequently, UV mediators must carry nontrivial flavor quantum numbers in order to couple consistently to SM fermions, with flavor invariance under G_F achieved through insertions of the SM

Yukawa matrices and Υ_ν [10].

For the mediator representations included here, the induced Wilson coefficients exhibit distinct spurionic suppression patterns, reflecting the transformation properties of the UV couplings under G_F . Among these possibilities, mediators transforming as $\mathbf{3}_q$ generically yield the least-suppressed contributions to all BNV operators generated at tree level. This makes the $\mathbf{3}_q$ assignment particularly relevant, as it provides UV completions whose

\mathcal{Q}_1 irreps	$g_{\mathcal{Q}_1}^{u\ell}$	$g_{\mathcal{Q}_1}^{dq}$	$\mathcal{O}_{duq\ell}$	$\mathcal{O}_{\ell u}$
$\mathbf{3}_q$	$[Y_u]^s{}_p[\mathcal{T}_\ell]_r$	$[Y_d^\dagger]^p{}_x \varepsilon^{sxxr}$	$\mathcal{O}(Y_u Y_d Y_e^2 \Upsilon_\nu)$	$\mathcal{O}(Y_u^2 Y_e^4 \Upsilon_\nu^2)$
$\mathbf{3}_u$	$\delta^s{}_p[\mathcal{T}_\ell]_r$	$[Y_u^\dagger]^s{}_x [Y_d^\dagger]^p{}_y \varepsilon^{xyr}$	$\mathcal{O}(Y_u Y_d Y_e^2 \Upsilon_\nu)$	$\mathcal{O}(Y_e^4 \Upsilon_\nu^2)$
$\overline{\mathbf{6}}_q$	$\varepsilon_{yx(s)} [Y_u Y_u^\dagger]^x {}_{ s'} [Y_u]^y{}_p [\mathcal{T}_\ell]_r$	$[Y_d^\dagger]^p{}_s \delta^r {}_{ s'}$	$\mathcal{O}(Y_u^3 Y_d Y_e^2 \Upsilon_\nu)$	$\mathcal{O}(Y_u^6 Y_e^4 \Upsilon_\nu^2)$
$(\mathbf{3}_q, \mathbf{3}_\ell)$	$[Y_u^\dagger]^s{}_p (\delta^{s'}{}_r + [\Upsilon_\nu \Upsilon_\nu^\dagger]^{s'}{}_r)$	$[\mathcal{T}_\ell^\dagger]^{s'} [Y_d^\dagger]^p{}_x \varepsilon^{sxxr}$	$\mathcal{O}(Y_u Y_d Y_e^2 \Upsilon_\nu)$	$\mathcal{O}(Y_u^2 \Upsilon_\nu^2)$
$(\mathbf{3}_u, \mathbf{3}_\ell)$	$\delta^s{}_p (\delta^{s'}{}_r + [\Upsilon_\nu \Upsilon_\nu^\dagger]^{s'}{}_r)$	$[\mathcal{T}_\ell^\dagger]^{s'} [Y_u^\dagger]^s{}_x [Y_d^\dagger]^p{}_y \varepsilon^{xyr}$	$\mathcal{O}(Y_u Y_d Y_e^2 \Upsilon_\nu)$	$\mathcal{O}(\Upsilon_\nu^2)$
$(\mathbf{3}_u, \overline{\mathbf{3}}_\ell)$	$\delta^s{}_p [\Upsilon_\nu^\dagger]_{s' r}$	$[\mathcal{T}_\ell]_{s'} [Y_u^\dagger]^s{}_x [Y_d^\dagger]^p{}_y \varepsilon^{xyr}$	$\mathcal{O}(Y_u Y_d Y_e^2 \Upsilon_\nu^2)$	$\mathcal{O}(\Upsilon_\nu^2)$
\mathcal{Q}_5 irreps	$g_{\mathcal{Q}_5}^{d\ell}$	$g_{\mathcal{Q}_5}^{eq}$	$\mathcal{O}_{duq\ell}$	\mathcal{O}_{qque}
$\mathbf{3}_q$	$[Y_d]^s{}_p[\mathcal{T}_\ell]_r$	$\delta^s{}_r[\mathcal{T}_e]_p$	$\mathcal{O}(Y_u Y_d Y_e^2 \Upsilon_\nu)$	$\mathcal{O}(Y_u Y_e^3 \Upsilon_\nu)$
$\mathbf{3}_d$	$\delta^s{}_p[\mathcal{T}_\ell]_r$	$[Y_d^\dagger]^s{}_r[\mathcal{T}_e]_p$	$\mathcal{O}(Y_u Y_d Y_e^2 \Upsilon_\nu)$	$\mathcal{O}(Y_u Y_d^2 Y_e^3 \Upsilon_\nu)$
$\overline{\mathbf{6}}_q$	$\varepsilon_{yx(s)} [Y_u Y_u^\dagger]^x {}_{ s'} [Y_d]^y{}_p [\mathcal{T}_\ell]_r$	$\varepsilon_{rx(s)} [Y_u Y_u^\dagger]^x {}_{ s'} [\mathcal{T}_e]_p$	$\mathcal{O}(Y_u^3 Y_d Y_e^2 \Upsilon_\nu)$	$\mathcal{O}(Y_u^3 Y_e^3 \Upsilon_\nu)$
$(\mathbf{3}_q, \mathbf{3}_\ell)$	$[Y_d]^s{}_p \delta^{s'}{}_r$	$\delta^s{}_r (\delta^{s'}{}_y + [\Upsilon_\nu \Upsilon_\nu^\dagger]^{s'}{}_y) [Y_e]^y{}_p$	$\mathcal{O}(Y_u Y_d Y_e^2 \Upsilon_\nu)$	$\mathcal{O}(Y_u Y_e^3 \Upsilon_\nu)$
$(\mathbf{3}_d, \mathbf{3}_\ell)$	$\delta^s{}_p \delta^{s'}{}_r$	$[Y_d^\dagger]^s{}_r (\delta^{s'}{}_y + [\Upsilon_\nu \Upsilon_\nu^\dagger]^{s'}{}_y) [Y_e]^y{}_p$	$\mathcal{O}(Y_u Y_d Y_e^2 \Upsilon_\nu)$	$\mathcal{O}(Y_u Y_d^2 Y_e^3 \Upsilon_\nu)$
$(\mathbf{3}_q, \overline{\mathbf{3}}_\ell)$	$[Y_d]^s{}_p [\Upsilon_\nu^\dagger]_{s' r}$	$\delta^s{}_r [\Upsilon_\nu^\dagger Y_e]_{s' p}$	$\mathcal{O}(Y_u Y_d Y_e^2 \Upsilon_\nu^2)$	$\mathcal{O}(Y_u Y_e^3 \Upsilon_\nu^2)$
\mathcal{Q}_5 irreps	$g_{\mathcal{Q}_5}^{uq}$		$\mathcal{O}_{qu}^{(1,8)}$	\mathcal{O}_{qe}
$\mathbf{3}_q$	$[Y_u^\dagger]^p{}_x \varepsilon^{sxxr}$		$\mathcal{O}(Y_u^2)$	$\mathcal{O}(Y_e^6 \Upsilon_\nu^2)$
$\mathbf{3}_d$	$[Y_u^\dagger]^p{}_x [Y_d^\dagger]^s{}_y \varepsilon^{xyr}$		$\mathcal{O}(Y_u^2 Y_d^2)$	$\mathcal{O}(Y_d^2 Y_e^6 \Upsilon_\nu^2)$
$\overline{\mathbf{6}}_q$	$[Y_d^\dagger]^p{}_s \delta^r {}_{ s'}$		$\mathcal{O}(Y_u^2)$	$\mathcal{O}(Y_u^4 Y_e^6 \Upsilon_\nu^2)$
$(\mathbf{3}_q, \mathbf{3}_\ell)$	$[\mathcal{T}_\ell^\dagger]^{s'} [Y_u^\dagger]^p{}_x \varepsilon^{sxxr}$		$\mathcal{O}(Y_u^2 Y_e^4 \Upsilon_\nu^2)$	$\mathcal{O}(Y_e^2 \Upsilon_\nu^2)$
$(\mathbf{3}_d, \mathbf{3}_\ell)$	$[\mathcal{T}_\ell^\dagger]^{s'} [Y_u^\dagger]^p{}_x [Y_d^\dagger]^s{}_y \varepsilon^{xyr}$		$\mathcal{O}(Y_u^2 Y_d^2 Y_e^4 \Upsilon_\nu^2)$	$\mathcal{O}(Y_d^2 Y_e^2 \Upsilon_\nu^2)$
$(\mathbf{3}_q, \overline{\mathbf{3}}_\ell)$	$[\mathcal{T}_\ell]_{s'} [Y_u^\dagger]^p{}_x \varepsilon^{sxxr}$		$\mathcal{O}(Y_u^2 Y_e^4 \Upsilon_\nu^2)$	$\mathcal{O}(Y_e^2 \Upsilon_\nu^2)$

TABLE 6. Overview of the leading spurionic invariants for the couplings of the vector leptoquarks \mathcal{Q}_1 and \mathcal{Q}_5 . The first column lists representative flavor representations of each LQ. The second and third columns display the flavor structures of the allowed renormalizable couplings to SM fermions, written in terms of the relevant flavor spurions (see Tab. 4 for details). The final two columns report the characteristic spurionic suppression of the SMEFT Wilson coefficients induced at tree level, both for the BNV operators and for a representative baryon-number-conserving operator entering $\mu - e$ conversion. The flavor indices p and r label the SM fermions appearing in the coupling tensors (two quarks for $g_{\mathcal{Q}_1}^{dq}$ and $g_{\mathcal{Q}_5}^{uq}$, and a quark-lepton pair for $g_{\mathcal{Q}_1}^{u\ell}$, $g_{\mathcal{Q}_5}^{d\ell}$, and $g_{\mathcal{Q}_5}^{eq}$). Each vector LQ carries either a single flavor index s when transforming in a fundamental representation of G_F , or a pair (s, s') when transforming as a sextet or a bifundamental. We employ the notation $2\psi_{(a|\chi|b)} = \psi_a \chi_b + \psi_b \chi_a$ to denote symmetrization over the indices a and b .

spurionic behavior aligns with the dominant structures identified in the EFT analysis of the previous section (see Tab. 1).

Beyond the fundamental $\mathbf{3}_f$ assignment, the extended MFV framework also allows the UV mediators to transform in $\overline{\mathbf{6}}_f$ and bifundamental representations, in particular of the form $(\mathbf{3}_q, \mathbf{3}_\ell)$ or $(\mathbf{3}_q, \overline{\mathbf{3}}_\ell)$, where f_q (f_ℓ) factor is associated with the quark (lepton) sector. By contrast, $\mathbf{8}_f$ representations are forbidden by group-theoretical considerations. The spurionic suppression arising from the bifundamental representations shows a more diverse structure compared to the fundamental assignment. For example, in the case of ω_1 mediator, the $(\mathbf{3}_q, \mathbf{3}_\ell)$ assignment generates contributions to the BNV operator \mathcal{O}_{qqql} with essentially the same spurionic scaling as the fundamental $\mathbf{3}_q$ representation. At the same time, the corresponding baryon-number-conserving operators, such as

$\mathcal{O}_{\ell q}^{(1,3)}$, may exhibit additional spurionic suppression, reflecting the need to contract both flavor indices of the bifundamental mediator through spurions belonging to different sectors. A similar pattern appears for the other LQ representations: while certain BNV operators induced by bifundamental representations retain a scaling comparable to the $\mathbf{3}_q$ case, the accompanying baryon-number-conserving operators typically exhibit a stronger degree of spurionic suppression.

It is noteworthy that some bifundamental representations introduce an additional layer of spurionic suppression for the BNV operators relative to the leading-order EFT treatment. This can be demonstrated by considering a few specific mediator assignments. For instance, adopting a UV completion in which the scalar mediators ω_1 or ζ transform as $(\mathbf{3}_q, \overline{\mathbf{3}}_\ell)$ leads to the bound of the

form

$$\Lambda_B \gtrsim 2 \text{ TeV} \left(\frac{\Lambda_L}{10^3 \text{ TeV}} \right), \quad (39)$$

which, when compared with the bound for $\mathcal{O}_{qq\ell}$ in Tab. 3, demonstrates the additional suppression introduced by extra insertion of Υ_ν , thereby further linking the proton-decay rate to the smallness of the neutrino masses.

Similarly, an even more pronounced example arises in the case of vector mediator \mathcal{Q}_1 transforming as $(\mathbf{3}_u, \bar{\mathbf{3}}_\ell)$, for which the bound reads

$$\Lambda_B \gtrsim 1 \text{ TeV} \left(\frac{\Lambda_L}{10^7 \text{ TeV}} \right), \quad (40)$$

which is substantially weaker than the corresponding limit for $\mathcal{O}_{duq\ell}$ in Tab. 3, again due to the enhanced suppression in Υ_ν .

These examples demonstrate how bifundamental assignments can introduce additional suppression, leading to weaker proton-decay bounds than those obtained in the minimally suppressed scenario. While such representations often entail more intricate UV dynamics and are less typical in minimal model-building approaches, they nonetheless demonstrate the importance of exploring explicit UV completions, as they can depart substantially from the expectations derived from the EFT spurion analysis alone.

In addition to the proton-decay limits, constraints on the baryon-number-conserving operators generated by these UV mediators provide a complementary probe of their parameter space. Current bounds obtained from the updated MFV SMEFT global fit of Ref. [68] typically place the scalar and vector LQs in the $1 - 3 \text{ TeV}$ mass range. Future sensitivities based on FCC projections without flavor assumptions [69, 70] are expected to extend this reach up to the $10 - 20 \text{ TeV}$ regime. Although these bounds provide useful complementary information, they are significantly weaker than those obtained from proton-decay searches, even when considering scenarios where additional spurion insertions reduce the latter.

Lastly, a further class of baryon-number-conserving observables is provided by cLFV processes, which are unavoidably induced once the lepton-sector spurions are switched on in the extended MFV framework. All five leptoquark mediators considered here generate the operators relevant for $\mu - e$ conversion in nuclei, whereas none of them induces the structures required for the $\mu \rightarrow 3e$ and $\mu \rightarrow e\gamma$ transitions at tree level. The corresponding amplitudes involve at least one insertion of the neutrino-mass spurion or the associated leptonic flavor invariants, and are therefore suppressed by the smallness of the neutrino masses and the charged-lepton Yukawas. As shown in App. B, the resulting limits offer complementary sensitivity to the leptonic spurion structure and to the flavor assignments of the mediators. However, throughout the parameter space relevant for our analysis, these cLFV

bounds remain well below those implied by proton-decay searches. They therefore serve primarily as a consistency check of the extended MFV framework, ensuring that the leptonic spurion structure implied by the UV completion remains compatible with existing limits on cLFV transitions.

V. REDUCED FLAVOR SYMMETRIES

Up to this point our analysis has relied on the extended MFV assumption, under which the full quark-lepton flavor symmetry is broken exclusively by the Yukawa matrices and the neutrino-mass spurion. Although MFV provides a coherent and systematically organized framework, its restrictiveness becomes apparent in the third-generation sector, where the large top Yukawa coupling induces a substantial breaking of the full G_F symmetry and may challenge the convergence of the spurion expansion. This observation has motivated increasing interest in flavor frameworks that relax MFV, particularly those in which new physics couples preferentially to third-generation fermions [37–40]. Such constructions arise naturally across several classes of UV models, ranging from supersymmetric models [37, 71, 72], composite Higgs setups [73–75], and more recently in flavor non-universal gauge theories [76–92]. These considerations motivate the exploration of flavor symmetries in which the full G_F structure is partially reduced. This section focuses on three representative realizations of reduced flavor symmetries: $U(2)^5$, $U(2)_{q,u}^2 \times U(3)_{d,\ell,e}^3$ and $U(2)_{q,u,d}^3 \times U(3)_{\ell,e}^2$.

In the following, we briefly characterize each of the reduced flavor-symmetry groups, specifying the transformation properties of the fermion fields and identifying the corresponding spurion structures. The present section does not attempt a full spurion analysis of the BNV operators or a derivation of the complete proton-decay bounds for each reduced-symmetry framework. Instead, we focus on the leading-order EFT structures permitted by these symmetries and examine how the reduced flavor assumptions modify the spurionic suppressions relative to extended MFV. This approach highlights the principal ways in which these frameworks depart from the MFV conclusions, both in the spurion hierarchies and in the resulting BNV amplitudes, providing a basis for assessing the phenomenological implications.

A. $U(2)^5$

A convenient starting point for reduced flavor symmetries is the $U(2)^5$ framework, in which the first two generations of each fermion species transform collectively as doublets while the third generation is treated as a singlet. Concretely, the flavor symmetry is taken to be

$$G_F \equiv U(2)_q \times U(2)_u \times U(2)_d \times U(2)_\ell \times U(2)_e, \quad (41)$$

Operator	Invariant	Component	Λ_B^{up} [TeV]	Λ_B^{down} [TeV]
$[\mathcal{O}_{qq\ell}]^{prst}$	$\frac{1}{\Lambda_B^2} \delta_{p3} \delta_{r3} \delta_{s3} \delta_{t3}$	S	2×10^9	2×10^8
	$\frac{1}{\Lambda_B^2} [\varepsilon_{pr} \delta_{s3} + \varepsilon_{sp} \delta_{r3} + \varepsilon_{rs} \delta_{p3}] \delta_{t3}$	A	1×10^{11}	1×10^{11}
	$\frac{1}{\Lambda_B^2} [\varepsilon_{pr} \delta_{s3} + \varepsilon_{sr} \delta_{p3}] \delta_{t3}$	M	3×10^{11}	2×10^{11}
$[\mathcal{O}_{duq\ell}]^{prst}$	$\frac{1}{\Lambda_B^2} \delta_{p3} \delta_{r3} \delta_{s3} \delta_{t3}$	-	4×10^8	3×10^7
$[\mathcal{O}_{qque}]^{prst}$	$\frac{1}{\Lambda_B^2} \delta_{p3} \delta_{r3} \delta_{s3} \delta_{t3}$	-	1×10^6	5×10^7
$[\mathcal{O}_{duee}]^{prst}$	$\frac{1}{\Lambda_B^2} \delta_{p3} \delta_{r3} \delta_{s3} \delta_{t3}$	S	1×10^7	1×10^7
	$\frac{1}{\Lambda_B^2} \delta_{p3} \varepsilon_{rs} \delta_{t3}$	A	2×10^7	2×10^7

TABLE 7. Dimension-six BNV SMEFT operators and the corresponding flavor-invariant structures in the $U(2)^5$ framework. The first column lists the relevant operator structures, while the second one denotes the corresponding $\mathcal{O}(1)$ flavor invariants. The third column specifies the operator component following the classification of Ref. [45], with S, A and M denoting the symmetric, antisymmetric, and mixed-symmetry components, respectively. The last two columns report the resulting lower bounds on Λ_B^{up} and Λ_B^{down} . All structures are predominantly constrained by the single proton-decay channel $p \rightarrow K^+ \nu$, in agreement with Ref. [32]. Decays into third-generation charged leptons are kinematically forbidden and can proceed only through off-shell τ exchange, which is far less constraining due to double Fermi constant insertions, additional phase-space suppression, and the comparatively weaker experimental sensitivities [31, 33, 35].

under which the quark and lepton fields decompose as $\psi = [\psi^a \ \psi_3]^\top$, with $a = 1, 2$ and $\psi = \{q, u, d, \ell, e\}$. Here ψ^a transforms as a doublet of the corresponding $U(2)_\psi$ factor, while ψ_3 is a singlet.

The breaking of $U(2)^5$ is parametrized by a minimal set of spurions that connect the doublet and singlet sectors and reproduce the observed fermion masses and mixing. In the quark sector, the breaking is encoded in a minimal set of spurions consisting of a doublet $V_q \sim \mathbf{2}_q$ linking the light and third generations, and two bifundamental 2×2 matrices $\Delta_{u,d} \sim (\mathbf{2}_q, \bar{\mathbf{2}}_{u,d})$, which encode the breaking within the first two generations of the up- and down-type sectors, respectively. Similarly, in the lepton sector the breaking of $U(2)_\ell \times U(2)_e$ is encoded in a single bifundamental spurion $\Delta_e \sim (\mathbf{2}_\ell, \bar{\mathbf{2}}_e)$.⁶ With this spurion content, the quark and charged-lepton Yukawa matrices take the block form [41]

$$Y_d = \begin{bmatrix} \Delta_d & 0 \\ 0 & y_b \end{bmatrix}, \quad Y_u = \begin{bmatrix} \Delta_u & V_q \\ 0 & y_t \end{bmatrix}, \quad Y_e = \begin{bmatrix} \Delta_e & 0 \\ 0 & y_\tau \end{bmatrix}, \quad (42)$$

where y_b , y_t , and y_τ denote the third-generation Yukawa couplings of the bottom quark, top quark, and tau lepton, respectively. A similar approach applies to the neutrino sector, in which the coefficient of the Weinberg operator in Eq. (5) gives rise to the LNV spurion Υ_ν , transforming as a symmetric tensor in lepton-flavor space. In the $U(2)^5$

framework, this spurion admits the block decomposition

$$\Upsilon_\nu = \begin{bmatrix} \Delta_\nu & V_\nu \\ V_\nu^\top & y_\nu \end{bmatrix}, \quad \Delta_\nu \sim \mathbf{3}_\ell, \quad V_\nu \sim \mathbf{2}_\ell, \quad y_\nu \in \mathbb{R}, \quad (43)$$

where Δ_ν corresponds to the symmetric triplet component arising from the decomposition $\mathbf{2} \otimes \mathbf{2} = \mathbf{3} \oplus \mathbf{1}$.

Having outlined the essential features of the $U(2)^5$ flavor framework, we now turn to its implications for the dimension-six BNV operators. Our approach is analogous to that adopted in the extended MFV framework: we construct the flavor invariants associated with each BNV operator, taking into account the intrinsic permutation symmetries of their Wilson coefficients. A key difference emerges already at this stage: contrary to MFV, where the absence of fermion-sector singlets forces every BNV structure to involve spurion insertions, the $U(2)^5$ symmetry admits fully $\mathcal{O}(1)$ flavor invariants constructed solely from the singlet components of the fermion fields. Consequently, leading BNV structures can be written without any spurion suppressions, provided they are consistent with the operator's internal symmetry relations. As a result, this directly implies significantly stronger bounds on Λ_B .

In the present analysis we focus on these $\mathcal{O}(1)$ contributions. Extending the construction to next-to-leading order would require insertions of the doublet spurions, and already at $\mathcal{O}(V_q)$ one finds sixteen additional independent structures. While such an extension is certainly feasible, it lies beyond the scope of this work. Phenomenologically, an immediate implication of the absence of spurion insertions is that the leading contributions do not depend on the LNV scale Λ_L , as no neutrino-sector spurions enter the construction. The resulting limits are

⁶ Note that a doublet spurion $V_\ell \sim \mathbf{2}_\ell$ may be introduced in general, but it is not needed in the minimal parametrization of the charged-lepton Yukawa matrix.

therefore expressed directly in terms of Λ_B , in contrast to the extended MFV case where the ratio $\mathcal{R}_{BL} = \Lambda_B^2/\Lambda_L$ is constrained. The complete set of leading $\mathcal{O}(1)$ flavor invariants for the dimension-six BNV operators, together with the resulting limits on Λ_B , is presented in Tab. 7. As anticipated, the absence of spurionic suppression leads to significantly stronger bounds on Λ_B than in the extended MFV case, where even the most favorable scenarios require $\Lambda_B \gtrsim 10^6$ TeV. Notably, in these scenarios proton decay is induced only at the two-loop level; nevertheless, this loop suppression alone is insufficient to lower the BNV scale to the multi-TeV regime [32].

The strength of these bounds, driven by the lack of spurionic suppression, provides a clear motivation to investigate other partially reduced flavor symmetries. Such frameworks may permit controlled suppressions of the BNV operators and thereby offer a more nuanced phenomenological picture, situated between the restrictive extended MFV case and the unsuppressed $U(2)^5$ limit. Accordingly, the remainder of the section will examine the intermediate frameworks $U(2)_{q,u}^2 \times U(3)_{d,\ell,e}^3$ and $U(2)_{q,u,d}^3 \times U(3)_{\ell,e}^2$, which represent concrete realizations of partially reduced flavor symmetries with distinct predicted suppression patterns.

Before concluding the discussion of the $U(2)^5$ framework, it is useful to comment briefly on the possible UV realizations of the leading BNV structures. Since $U(2)^5$ admits fermion singlets, all unsuppressed $\mathcal{O}(1)$ flavor invariants identified in Tab. 7 can be generated by appropriate UV mediators transforming as flavor singlets. As a concrete illustration, a scalar mediator such as ω_1 , when taken to transform as a singlet under $U(2)^5$, can induce the symmetric component of \mathcal{O}_{duee} . Likewise, a singlet ω_4 , whose up-type coupling $[y_{\omega_4}^{uu}]^{pr}$ is intrinsically antisymmetric, naturally generates the antisymmetric component of the same operator.

Additionally, beyond singlet assignments, one may also consider UV mediators transforming in nontrivial representations of $U(2)^5$. In such cases, flavor invariance requires the renormalizable interactions to involve the appropriate spurion insertions. For instance, if ω_4 transforms as $\mathbf{2}_u$, the coupling to two up-type quarks can be written as $[y_{\omega_4}^{uu}]^{spr} = (\Delta_u^\dagger V_q)^s \varepsilon^{pr}$, while the right-handed leptons and down quarks is given by $[y_{\omega_4}^{ed}]^s_{pr} = (\Delta_u^\dagger V_q)^s \delta_{p3} \delta_{r3}$. Integrating out the mediator in this flavor representation at tree level generates the BNV operator \mathcal{O}_{duee} with coefficient $[\mathcal{C}_{duee}]_{prst} \sim (V_q^\dagger \Delta_u)(\Delta_u^\dagger V_q) \delta_{p3} \varepsilon_{rs} \delta_{t3}$, which is suppressed by $\mathcal{O}(V_q^2 \Delta_u^2)$ [62]. Numerically, one finds $(V_q^\dagger \Delta_u)(\Delta_u^\dagger V_q) \simeq 10^{-8}$ [41], implying a corresponding lower bound on the mediator mass of $M_{\omega_4} \gtrsim 1.5 \times 10^3$ TeV.

B. $U(2)_{q,u,d}^3 \times U(3)_{\ell,e}^2$ and $U(2)_{q,u}^2 \times U(3)_{d,\ell,e}^3$

We next consider two intermediate flavor symmetries that interpolate between the $U(2)^5$ and extended MFV

construction, namely $U(2)_{q,u,d}^3 \times U(3)_{\ell,e}^2$ and $U(2)_{q,u}^2 \times U(3)_{d,\ell,e}^3$. The first symmetry choice is fully specified by the $U(2)^3$ spurions in the quark sector (see Eq. (42)) together with the $U(3)^2$ lepton-sector assignments specified in Sec. II. The construction of the BNV flavor invariants in the quark sector proceeds exactly as in the $U(2)^5$ case, while, in contrast, the invariance under $U(3)_{\ell,e}^2$ is achieved through the inclusion of the appropriate lepton-sector spurions. Consequently, the lepton-sector invariants necessarily acquire spurion suppressions leading to a characteristic scaling with the neutrino masses.

The second framework of interest involves $U(2)_{q,u}^2 \times U(3)_{d,\ell,e}^3$ symmetry. Restoring $U(3)_d$ symmetry has an immediate consequence for the spurion content: since q and u retain their $U(2)$ transformation properties, whereas d now transforms as a $U(3)_d$ triplet, the symmetry breaking is controlled by three spurions, in particular, $\Delta_u \sim (\mathbf{2}_q, \bar{\mathbf{2}}_u)$, $\Sigma_d \sim (\mathbf{2}_q, \bar{\mathbf{3}}_d)$ and $\Lambda_d \sim \mathbf{3}_d$.⁷ With this spurion content, the minimal parametrization of the quark Yukawa matrices takes the form [41]

$$Y_u = \begin{bmatrix} \Delta_u & 0 \\ 0 & y_t \end{bmatrix}, \quad Y_d = \begin{bmatrix} \Sigma_d \\ \Lambda_d^\dagger \end{bmatrix}, \quad y_t \in \mathbb{R}. \quad (44)$$

Restoring $U(3)_d$ further implies that any BNV operator involving down quarks requires insertion of the $\Lambda_d \simeq 10^{-2}$ spurion, introducing additional suppression compared to the previous case.

The resulting flavor-invariant structures for both symmetry assumptions, together with the corresponding decay channels and bounds on the ratio Λ_B^2/Λ_L , are collected in Tab. 8. In addition to the entries shown, it is worth noting that several operators give rise to multiple proton-decay channels with comparable sensitivity.

For the $U(2)_{q,u,d}^3 \times U(3)_{\ell,e}^2$ symmetry, the operator \mathcal{O}_{qque} in the down basis is constrained not only by the quoted $p \rightarrow K^0 \mu^+$ channel but also by $p \rightarrow \pi^0 \mu^+$ and $p \rightarrow K^+ \nu$, which provide limits of similar strength. Likewise, the bounds on the antisymmetric component of \mathcal{O}_{duee} (in both the up and down bases) are accompanied by the mode $p \rightarrow K^0 \mu^+$, again yielding comparable sensitivity. Lastly, for the antisymmetric component of \mathcal{O}_{qqql} in the down basis, the quoted $p \rightarrow K^+ \nu$ constraint is representative of a broader set of channels exhibiting similar reach.

A similar situation occurs in the $U(2)_{q,u}^2 \times U(3)_{d,\ell,e}^3$ framework. For the antisymmetric component of \mathcal{O}_{duee} , the channel $p \rightarrow K^0 \mu^+$ provides constraints comparable to those from $p \rightarrow \pi^0 \mu^+$. The operator \mathcal{O}_{duql} in the down basis receives contributions from several additional modes, including $p \rightarrow K^0 e^+$, $p \rightarrow K^+ \nu$, $p \rightarrow \eta^0 e^+$, and $p \rightarrow K^0 \mu^+$, all of which probe similar scales. Similarly,

⁷ A doublet spurion $V_q \sim \mathbf{2}_q$ may be included to account for additional mixing between the third generation and the light quarks, but it is not required for the minimal parametrization of the Yukawa matrices.

Operator	Spurion expansion	Component	$\mathcal{R}_{\text{BL}}^{\text{up}}$ [TeV]	Channel	$\mathcal{R}_{\text{BL}}^{\text{down}}$ [TeV]	Channel
$[\mathcal{O}_{qqq\ell}]^{prst}$	$\frac{1}{\Lambda_B^2} \delta_{p3} \delta_{r3} \delta_{s3} [\mathcal{T}_\ell]_t$	S	80	$p \rightarrow K^+ \nu$	7	$p \rightarrow \pi^0 e^+$
	$\frac{1}{\Lambda_B^2} [\varepsilon_{pr} \delta_{s3} + \varepsilon_{sp} \delta_{r3} + \varepsilon_{rs} \delta_{p3}] [\mathcal{T}_\ell]_t$	A	10^7	$p \rightarrow K^+ \nu$	10^7	$p \rightarrow K^+ \nu$
	$\frac{1}{\Lambda_B^2} [\varepsilon_{pr} \delta_{s3} + \varepsilon_{sr} \delta_{p3}] [\mathcal{T}_\ell]_t$	M	10^7	$p \rightarrow K^+ \nu$	9×10^6	$p \rightarrow K^+ \nu$
$[\mathcal{O}_{duq\ell}]^{prst}$	$\frac{1}{\Lambda_B^2} \delta_{p3} \delta_{r3} \delta_{s3} [\mathcal{T}_\ell]_t$	-	1	$p \rightarrow K^+ \nu$	10^{-1}	$p \rightarrow \pi^0 e^+$
$[\mathcal{O}_{qque}]^{prst}$	$\frac{1}{\Lambda_B^2} \delta_{p3} \delta_{r3} \delta_{s3} [\mathcal{T}_\ell]_t$	-	10^{-4}	$p \rightarrow K^+ \nu$	10^{-1}	$p \rightarrow K^0 \mu^+$
$[\mathcal{O}_{duue}]^{prst}$	$\frac{1}{\Lambda_B^2} \delta_{p3} \delta_{r3} \delta_{s3} [\mathcal{T}_e]_t$	S	10^{-8}	$p \rightarrow K^+ \nu$	10^{-8}	$p \rightarrow K^+ \nu$
	$\frac{1}{\Lambda_B^2} \delta_{p3} \varepsilon_{rs} [\mathcal{T}_e]_t$	A	6×10^{-4}	$p \rightarrow \pi^0 \mu^+$	6×10^{-4}	$p \rightarrow \pi^0 \mu^+$
	$\frac{1}{\Lambda_B^2} \delta_{p3} \delta_{r3} \delta_{s3} [\mathcal{T}_\ell]_t$	S	80	$p \rightarrow K^+ \nu$	7	$p \rightarrow \pi^0 e^+$
$[\mathcal{O}_{qqq\ell}]^{prst}$	$\frac{1}{\Lambda_B^2} [\varepsilon_{pr} \delta_{s3} + \varepsilon_{sp} \delta_{r3} + \varepsilon_{rs} \delta_{p3}] [\mathcal{T}_\ell]_t$	A	10^7	$p \rightarrow K^+ \nu$	10^7	$p \rightarrow K^+ \nu$
	$\frac{1}{\Lambda_B^2} [\varepsilon_{pr} \delta_{s3} + \varepsilon_{sr} \delta_{p3}] [\mathcal{T}_\ell]_t$	M	10^7	$p \rightarrow K^+ \nu$	9×10^6	$p \rightarrow K^+ \nu$
$[\mathcal{O}_{duq\ell}]^{prst}$	$\frac{1}{\Lambda_B^2} [\Lambda_d^\dagger]_p \delta_{r3} \delta_{s3} [\mathcal{T}_\ell]_t$	-	2×10^{-2}	$p \rightarrow K^+ \nu$	4×10^{-3}	$p \rightarrow \pi^0 e^+$
$[\mathcal{O}_{qque}]^{prst}$	$\frac{1}{\Lambda_B^2} \delta_{p3} \delta_{r3} \delta_{s3} [\mathcal{T}_e]_t$	-	10^{-4}	$p \rightarrow K^+ \nu$	10^{-1}	$p \rightarrow K^0 \mu^+$
$[\mathcal{O}_{duue}]^{prst}$	$\frac{1}{\Lambda_B^2} [\Lambda_d^\dagger]_p \delta_{r3} \delta_{s3} [\mathcal{T}_e]_t$	S	10^{-10}	$p \rightarrow K^+ \nu$	10^{-10}	$p \rightarrow K^+ \nu$
	$\frac{1}{\Lambda_B^2} [\Lambda_d^\dagger]_p \varepsilon_{rs} [\mathcal{T}_e]_t$	A	7×10^{-6}	$p \rightarrow \pi^0 \mu^+$	7×10^{-6}	$p \rightarrow \pi^0 \mu^+$

TABLE 8. Dimension-six BNV SMEFT operators and the corresponding flavor-invariant structures for the $U(2)_{q,u,d}^3 \times U(3)_{\ell,e}^2$ (upper panel) and $U(2)_{q,u}^2 \times U(3)_{d,\ell,e}^3$ (lower panel) framework. The first column lists the relevant operator structures, while the second displays the least suppressed spurion insertions required to render each operator invariant under the full flavor symmetry group. The third column specifies the operator component following the classification of Ref. [45], with S, A and M denoting the symmetric, antisymmetric, and mixed-symmetry components, respectively. The fourth (sixth) column reports the bounds on the ratio $\mathcal{R}_{\text{BL}} \equiv \Lambda_B^2 / \Lambda_L$ in the up (down) basis, denoted as $\mathcal{R}_{\text{BL}}^{\text{up}}$ ($\mathcal{R}_{\text{BL}}^{\text{down}}$), while the adjacent columns indicate the decay channel that provides the most stringent limit in each case.

the antisymmetric component of $\mathcal{O}_{qqq\ell}$ in the down basis yields a variety of competitive channels, such as $p \rightarrow K^0 e^+$, $p \rightarrow \pi^0 e^+$, $n \rightarrow K^0 \nu$, $p \rightarrow \eta^0 e^+$, and $p \rightarrow K^0 \mu^+$.

Finally, for both flavor assumptions, the constraint arising from the fully symmetric component of $\mathcal{O}_{qqq\ell}$ is weaker by about three orders of magnitude relative to those obtained from the antisymmetric or mixed components. This reduction stems from the fact that the symmetric structure involves only third-generation quarks and contributes to proton decay only at two loops, leading to a parametrically suppressed rate [32].

Taken together, the two intermediate flavor frameworks yield proton-decay limits that allow a multi-TeV BNV scale for all dimension-six operators aside from $\mathcal{O}_{qqq\ell}$, consistent with the pattern observed in the MFV analysis. The bounds associated with $\mathcal{O}_{qqq\ell}$ and \mathcal{O}_{qque} closely track their MFV counterparts, whereas those for $\mathcal{O}_{duq\ell}$ and \mathcal{O}_{duue} are enhanced (reduced) by about an order of magnitude in the $U(2)_{q,u,d}^3 \times U(3)_{\ell,e}^2$ ($U(2)_{q,u}^2 \times U(3)_{d,\ell,e}^3$) framework, where the weakening in the latter case follows from the additional insertion of the down-sector spurion Λ_d .

As a final point, we note that the leading BNV struc-

tures listed in Tab. 8 can, as in the $U(2)^5$ case, be generated by flavor-singlet UV mediators, in contrast to extended MFV where mediators need to transform in non-trivial flavor representations. From a model-building perspective, this makes the present flavor assumptions considerably simpler than in the MFV case. Allowing non-singlet mediators again yields subleading, spurion-suppressed contributions.

VI. CONCLUSIONS

The hierarchical pattern of fermion masses and mixings in the SM suggests that flavor symmetries may play an essential role in structuring new physics, as emphasized in MFV and related frameworks. Proton decay, in turn, offers a uniquely sensitive probe of BNV and constitutes one of the clearest possible signals of physics beyond the SM. Previous work examined BNV within MFV settings [12, 13], showing that the scale of new physics mediating BNV can be lowered by many orders of magnitude relative to the naive expectation $\Lambda_B \gtrsim 10^{16}$ GeV, though these works relied on schematic estimates rather

than a full phenomenological analysis.

In this work we carried out a detailed EFT analysis of BNV under several flavor-symmetry assumptions within the SMEFT framework. In the MFV case, we confirmed the unavoidable link between BNV and LNV, showing that proton-decay amplitudes acquire a characteristic suppression proportional to m_ν^2 . This relation both explains why the BNV scale Λ_B may lie far below the naive expectation and implies that an eventual observation of proton decay would indirectly point to a Majorana origin of neutrino masses.

For each of the four independent dimension-six BNV operators, we derived bounds on Λ_B (and their implicit dependence on the LNV scale Λ_L) and identified the dominant decay channels. Our analysis combines a full numerical SMEFT-LEFT evolution supplemented with an analytic leading-log discussion, further clarifying the origin of relevant effects. We show that the operator \mathcal{O}_{qqql} generates proton decay at tree level and thus yields the strongest bounds, whereas, \mathcal{O}_{duql} , \mathcal{O}_{qque} and \mathcal{O}_{duue} allow for much weaker limits. Aside from \mathcal{O}_{qqql} , all operators remain compatible with Λ_B in the multi-TeV range for suitable choices of Λ_L . We note that the required values for Λ_L may lie well below the naive expectation for type-I seesaw scale, while remaining naturally accommodated in type-II or inverse seesaw realizations. Finally, we identified correlations among the dominant proton-decay channels that depend only on Λ_B , allowing potential future measurements to discriminate which dimension-six BNV operator is preferred.

Beyond the EFT analysis, we also examined the set of possible single-particle UV completions. In the MFV framework, such mediators necessarily transform non-trivially under the flavor group, and certain representations were found to introduce an additional spurionic suppression, enhancing the neutrino-mass dependence to $\Gamma_p \propto m_\nu^4$. While these constructions are not meant to represent the fully developed UV scenarios, they serve to illustrate how going beyond a leading-order EFT description can open qualitatively different possibilities.

In addition, we explored several reduced flavor assumptions. Starting with the $U(2)^5$ framework, at leading order, proton decay no longer inherits the neutrino-mass suppression present in MFV, leading to substantially stronger bounds on the BNV scale. In turn, the intermediate symmetries $U(2)_{q,u,d}^3 \times U(3)_{\ell,e}^2$ and $U(2)_{q,u}^2 \times U(3)_{d,\ell,e}^3$ restore the MFV-like suppression pattern and permit multi-TeV values of Λ_B . These frameworks additionally permit flavor-singlet UV mediators for the leading BNV structures, offering simpler UV completions.

Looking ahead, the present analysis suggests several directions for future work. From a phenomenological perspective, a natural next step involves broadening the EFT treatment beyond the leading structures considered here, as well as extending the study to higher-dimensional BNV operators, which can mediate qualitatively distinct effects. In parallel, another complementary direction involves exploring more complete UV realizations beyond

the minimal setups discussed in this work.

In conclusion, we have shown that the interplay between flavor symmetries and BNV yields a rich and predictive structure, with direct implications for proton-decay searches, offering clear criteria for interpreting possible future signals. Upcoming experimental advances are expected to provide further valuable insights into these underlying mechanisms.

Acknowledgments. We thank Juan Herrero-García and Andreas Crivellin for helpful discussions, and John Gargalionis and Arcadi Santamaria for reading the manuscript. ABB also thanks the University of Basel and Prof. Admir Greljo’s group, and to the Università di Padova and INFN Sezione di Padova, for their warm hospitality at the various stages of this project. ABB also expresses gratitude to the University of Basel, and to the Università di Padova and INFN Sezione di Padova, for their warm hospitality during various stages of this project. The work of ABB is funded by the grant CIACIF/2021/061 of the “Generalitat Valenciana” and also by the Spanish “Agencia Estatal de Investigación” through MICIN/AEI/10.13039/501100011033. The work of AP is supported by the Excellence Severo Ochoa project CEX2023-001292-S (MCIU/AEI/10.13039/501100011033). The work of AS received funding from the INFN Iniziativa Specifica APINE.

Appendix A: Group Theory of Flavor Invariants

This appendix presents the group-theoretical construction of lepton and quark flavor invariants in the extended MFV framework, with emphasis on identifying the least-suppressed invariant structures.

1. Lepton Sector

We consider the subgroup $G_F \supset U(3)_\ell \times U(3)_e$, under which the SM lepton fields transform canonically as triplets under the corresponding $U(3)$ factors. The relevant spurions are the charged-lepton Yukawa matrix $Y_e \sim (\mathbf{3}_\ell, \bar{\mathbf{3}}_e)$, and the symmetric neutrino mass spurion $\Upsilon_\nu \sim \mathbf{6}_\ell$. To identify the leading MFV structures, we examine the allowed flavor-singlet contractions formed from the spurions and the lepton fields. Since each dimension-six BNV operator includes only one lepton-field insertion, the ℓ and e contractions are treated separately.

For $\ell \sim \mathbf{3}_\ell$, starting with the decomposition of the form

$$Y_e Y_e^\dagger \sim (\mathbf{1}, \mathbf{1}) \oplus (\mathbf{8}_\ell, \mathbf{1}) \oplus (\mathbf{1}, \mathbf{8}_e) \oplus (\mathbf{8}_\ell, \mathbf{8}_e), \quad (\text{A1})$$

it follows that the $(Y_e Y_e^\dagger) \ell$ product contains

$$(Y_e Y_e^\dagger) \ell \supset \mathbf{8}_\ell \otimes \mathbf{3}_\ell = \mathbf{3}_\ell \oplus \bar{\mathbf{6}}_\ell \oplus \mathbf{15}_\ell. \quad (\text{A2})$$

Lastly, taking the tensor product of this structure with the $\Upsilon_\nu \sim \mathbf{6}_\ell$ yields

$$\Upsilon_\nu (Y_e Y_e^\dagger) \ell \supset \mathbf{6}_\ell \otimes (\mathbf{3}_\ell \oplus \bar{\mathbf{6}}_\ell \oplus \mathbf{15}_\ell) \supset \mathbf{6}_\ell \otimes \bar{\mathbf{6}}_\ell \supset \mathbf{1}. \quad (\text{A3})$$

Following these decompositions, the least suppressed flavor invariant reads

$$\mathcal{I}_F^\ell \sim \varepsilon_{prs} [\Upsilon_\nu]^{pt} [Y_e^\dagger]^m{}_t [Y_e]^r{}_m \ell^s, \quad (\text{A4})$$

with the contractions in flavor space made explicit.

In case of $e \sim \mathbf{3}_e$, following the similar approach as for the ℓ case, our starting point is the decomposition

$$Y_e^\dagger Y_e^\dagger \sim (\mathbf{3}_\ell, \bar{\mathbf{3}}_e) \oplus (\mathbf{3}_\ell, \mathbf{6}_e) \oplus (\bar{\mathbf{6}}_\ell, \bar{\mathbf{3}}_e) \oplus (\bar{\mathbf{6}}_\ell, \mathbf{6}_e), \quad (\text{A5})$$

from which we can write

$$Y_e^\dagger Y_e^\dagger e \supset (\bar{\mathbf{6}}_\ell, \bar{\mathbf{3}}_e) \otimes \mathbf{3}_e \supset (\bar{\mathbf{6}}_\ell, \mathbf{1}). \quad (\text{A6})$$

Lastly, contracting with Υ_ν , we obtain

$$\Upsilon_\nu Y_e^\dagger Y_e^\dagger e \supset \mathbf{6}_\ell \otimes (\bar{\mathbf{6}}_\ell, \mathbf{1}) \supset \mathbf{1}. \quad (\text{A7})$$

With these decompositions in mind, the flavor invariant takes the form

$$\mathcal{I}_F^e \sim [\Upsilon_\nu]^{pr} \varepsilon_{stm} [Y_e^\dagger]^s{}_p [Y_e^\dagger]^t{}_r e^m, \quad (\text{A8})$$

where $2\psi_{(a|\chi|b)} = \psi_a \chi_b + \psi_b \chi_a$ denotes the symmetrized sum. However, as can be seen from Eq. (A8), the contraction involves an antisymmetric tensor ε_{stm} together with a spurion combination that is symmetric under the exchange $s \leftrightarrow t$. As a result, the entire expression vanishes identically. This observation is consistent with the findings of Ref. [12], which notes that BNV operators involving e fields are more suppressed by flavor considerations than those involving ℓ . Our derivation, however, is based on an explicit group-theoretical analysis and operator construction. Furthermore, this implies that constructing a non-vanishing invariant necessitates the insertion of an additional spurion, leading to a minimally suppressed structure that can be written as

$$\mathcal{I}_F^e \sim \varepsilon_{prs} [\Upsilon_\nu]^{pt} [Y_e^\dagger]^m{}_t [Y_e]^r{}_m [Y_e]^s{}_n e^n. \quad (\text{A9})$$

Given that the purely leptonic spurion structures defined in Eqs. (A4) and (A9) systematically enter the construction of BNV operators within the extended MFV framework (see Sec. III A), we introduce the following shorthand notation in order to streamline the presentation of these recurrent combinations

$$[\mathcal{T}_\ell]_s \equiv \varepsilon_{prs} [\Upsilon_\nu]^{pt} [Y_e Y_e^\dagger]^r{}_t \sim \bar{\mathbf{3}}_\ell, \quad (\text{A10})$$

and

$$[\mathcal{T}_e]_n \equiv \varepsilon_{prs} [\Upsilon_\nu]^{pt} [Y_e Y_e^\dagger]^r{}_t [Y_e]^s{}_n \sim \bar{\mathbf{3}}_e. \quad (\text{A11})$$

The flavor invariants derived in this section have been independently verified using the `Sym2Int` package [93, 94].

Lastly, we summarize the numerical inputs relevant for the lepton-sector invariants. Using the parametrization of Υ_ν in terms of current neutrino-oscillation parameters detailed in Sec. II, along with the measured values for the charged-lepton Yukawa matrix, we find the following numerical values for \mathcal{T}_ℓ in the Normal Ordering (NO) and Inverted Ordering (IO)

$$\begin{aligned} \mathcal{T}_\ell^{\text{NO}} &= \frac{\Lambda_L}{\text{TeV}} \begin{bmatrix} 7.2 \\ 2.5 \\ (-3+i) \times 10^{-3} \end{bmatrix} \times 10^{-17}, \\ \mathcal{T}_\ell^{\text{IO}} &= \frac{\Lambda_L}{\text{TeV}} \begin{bmatrix} -8.3 + 0.1i \\ -1.5 - 0.5i \\ (7+2i) \times 10^{-3} \end{bmatrix} \times 10^{-17}, \end{aligned} \quad (\text{A12})$$

while for the additionally spurion-suppressed \mathcal{T}_e we find

$$\begin{aligned} \mathcal{T}_e^{\text{NO}} &= \frac{\Lambda_L}{\text{TeV}} \begin{bmatrix} 0.02 \\ 1.5 - 0.2i \\ -0.03 \end{bmatrix} \times 10^{-20}, \\ \mathcal{T}_e^{\text{IO}} &= \frac{\Lambda_L}{\text{TeV}} \begin{bmatrix} -0.2 \\ -9.0 - 2.9i \\ 0.7 + 0.2i \end{bmatrix} \times 10^{-21}. \end{aligned} \quad (\text{A13})$$

As input parameters, we use the central values from the latest global fit to neutrino-oscillation data [44], together with the most recent PDG determinations of the charged-lepton masses [50].

2. Quark Sector

The construction of flavor invariants in the quark sector proceeds in close analogy with the lepton-sector analysis. The similar group-theoretical logic applies, with the spurion content now involving the two quark Yukawa matrices $Y_{u,d} \sim (\mathbf{3}_q, \bar{\mathbf{3}}_{u,d})$, and all contractions need to be invariant under the quark subgroup $G_F \supset \text{U}(3)_q \times \text{U}(3)_u \times \text{U}(3)_d$.

We start by classifying the structures generated by two spurion insertions

$$\begin{aligned} Y_u Y_u^\dagger &\sim (\mathbf{1}, \mathbf{1}) \oplus (\mathbf{8}_q, \mathbf{1}) \oplus (\mathbf{1}, \mathbf{8}_u) \oplus (\mathbf{8}_q, \mathbf{8}_u), \\ Y_u Y_u &\sim (\bar{\mathbf{3}}_q, \mathbf{3}_u) \oplus (\mathbf{6}_q, \mathbf{3}_u) \oplus (\bar{\mathbf{3}}_q, \bar{\mathbf{6}}_u) \oplus (\mathbf{6}_q, \bar{\mathbf{6}}_u), \\ Y_u Y_d^\dagger &\sim (\mathbf{1}, \bar{\mathbf{3}}_u \otimes \mathbf{3}_d) \oplus (\mathbf{8}_q, \bar{\mathbf{3}}_u \otimes \mathbf{3}_d), \\ Y_u Y_d &\sim (\bar{\mathbf{3}}_q, \bar{\mathbf{3}}_u \otimes \bar{\mathbf{3}}_d) \oplus (\mathbf{6}_q, \bar{\mathbf{3}}_u \otimes \bar{\mathbf{3}}_d). \end{aligned} \quad (\text{A14})$$

The remaining structures follow straightforwardly by taking conjugates or by substituting $u \rightarrow d$. We further note the additional decompositions that prove useful in constructing the invariants

$$\begin{aligned} \mathbf{8} \otimes \mathbf{3} &= \mathbf{3} \oplus \bar{\mathbf{6}} \oplus \mathbf{15}, & \mathbf{6} \otimes \mathbf{3} &= \mathbf{8} \oplus \mathbf{10}, \\ \mathbf{8} \otimes \bar{\mathbf{3}} &= \bar{\mathbf{3}} \oplus \mathbf{6} \oplus \bar{\mathbf{15}}, & \mathbf{6} \otimes \bar{\mathbf{3}} &= \mathbf{3} \oplus \mathbf{15}. \end{aligned} \quad (\text{A15})$$

These decompositions provide the building blocks for assembling all relevant flavor invariants, both at the operator level within SMEFT and in the corresponding UV

interactions.

At the operator level, this procedure can be illustrated using the example of $\mathcal{O}_{qqq\ell}$, which contains three insertions of $q \sim \mathbf{3}_q$. At leading order, the flavor contraction follows from the decomposition

$$\mathbf{3}_q \otimes \mathbf{3}_q \otimes \mathbf{3}_q = \mathbf{3}_q \otimes (\mathbf{6}_q \oplus \bar{\mathbf{3}}_q) \supset \mathbf{3}_q \otimes \bar{\mathbf{3}}_q = \mathbf{1} \oplus \mathbf{8}_q, \quad (\text{A16})$$

so a flavor singlet can be formed directly using the invariant tensor ε_{prs} . At next-to-leading order in the spurion expansion, another invariant can be formed by inserting $Y_u Y_u^\dagger \supset (\mathbf{8}_q, \mathbf{1})$. Selecting the adjoint $\mathbf{8}_q$ component, the decomposition

$$\mathbf{3}_q \otimes \mathbf{3}_q \otimes \mathbf{3}_q \supset \mathbf{3}_q \otimes \mathbf{6}_q \supset \mathbf{8}_q \quad (\text{A17})$$

provides an octet that can be contracted with the octet from $Y_u Y_u^\dagger$ to form a singlet. With the explicit contractions in the flavor space, this invariant reads $\mathcal{I}_F^{qqq} \sim \varepsilon_{prx} [Y_u Y_u^\dagger]^x_s$.

A similar group-theoretical strategy applies to operators involving quarks in different flavor representations. For instance, $\mathcal{O}_{duq\ell}$, which transforms as $\mathbf{3}_d \otimes \mathbf{3}_u \otimes \mathbf{3}_q$, does not admit a flavor singlet at leading order. However, at next-to-leading order the decomposition of product $Y_u Y_d$ contains a $(\mathbf{3}_q, \mathbf{3}_u \otimes \bar{\mathbf{3}}_d)$ component, which combines with $\mathcal{O}_{duq\ell} \sim \mathbf{3}_d \otimes \mathbf{3}_u \otimes \mathbf{3}_q$ to produce a flavor singlet. The flavor invariant then reads $\mathcal{I}_F^{duq} \sim \varepsilon_{abs} [Y_u]^a_r [Y_d]^b_p$.

Furthermore, flavor invariants involving the UV mediators are obtained in complete analogy with those constructed at the operator level. In this context, if the UV mediator transforms as a flavor singlet, no invariant involving a single quark field can be formed. Indeed, a quark transforming as $\mathbf{3}_x$ with $x \in \{q, u, d\}$ would require a compensating spurion in the conjugate representation $\bar{\mathbf{3}}_x$, which cannot be generated from quark Yukawa insertions alone. Since Yukawa matrices transform as bifundamentals, any combination of them yields representations containing an even number of fundamental indices. This conclusion is also not altered by determinant insertions, as the symmetrization of two Yukawa matrices of the same type removes the would-be $\mathbf{3}_x$ spurion.

To this end, a useful illustration is obtained by introducing a new spurion Ω (representing a UV mediator) transforming in a nontrivial quark-flavor representation and asking under which conditions a flavor-singlet object involving a single quark field can be constructed. If $\Omega \sim \mathbf{3}_x$ with $x \in \{q, u, d\}$, the construction is straightforward: a single insertion of the appropriate Yukawa matrix suffices to form an invariant. On the other hand, for $\Omega \sim \mathbf{6}_q$ the relevant decomposition becomes

$$\Omega (Y_u Y_u^\dagger) q \supset \mathbf{6}_q \otimes (\mathbf{8}_q \otimes \mathbf{3}_q) \supset \mathbf{6}_q \otimes \bar{\mathbf{6}}_q \supset \mathbf{1}, \quad (\text{A18})$$

where we select the adjoint component of $Y_u Y_u^\dagger$ product. Similarly, for $\Omega \sim \mathbf{6}_x$ with $x \in \{u, d\}$, singlet constructions remain possible, although they may require additional Yukawa insertions.

Next, considering the case $\Omega \sim \mathbf{8}_q$, one finds that no flavor singlet can be built from a single insertion of $q \sim \mathbf{3}_q$, even after allowing for two Yukawa insertions. As follows from the decompositions given by Eq. (A15), the products $\mathbf{8}_q \otimes \mathbf{3}_q$ and $\mathbf{8}_q \otimes \bar{\mathbf{3}}_q$ contain no singlet. Moreover, extracting an octet from $Y_{u,d} Y_{u,d}^\dagger$ does not alter this conclusion, since the subsequent tensor products likewise fail to yield a singlet. A similar argument applies when considering three Yukawa insertions. From the decomposition of $Y_{u,d}^3$, one may isolate the $Y_{u,d}^3 \supset (\mathbf{3}_q \otimes \mathbf{3}_q \otimes \mathbf{3}_q, \mathbf{1})$ components, where the singlet arises through fully antisymmetric ε -contractions in the u - or d -sector. However, on the q -side the relevant products $\mathbf{3}_q \otimes \mathbf{3}_q \otimes \mathbf{3}_q \otimes \mathbf{3}_q$ and $\mathbf{3}_q \otimes \mathbf{3}_q \otimes \mathbf{3}_q \otimes \bar{\mathbf{3}}_q$ contain no $\mathbf{8}_q$ representation that could be paired with $\Omega \sim \mathbf{8}_q$. As a consequence, even allowing for three Yukawa insertions, no flavor singlet involving a single q field can be formed when Ω transforms as a flavor octet. Similar reasoning applies to $\Omega \sim \mathbf{8}_x$ with $x \in \{u, d\}$, where no singlet constructions are possible.

Appendix B: Extended MFV and cLFV

Charged-lepton flavor violation (cLFV) arises in the extended MFV framework through the same leptonic spurions that enter the BNV analysis. In the SM these effects are suppressed by neutrino masses, so any observable signal would be a clear indication of new physics. This appendix summarizes the leading MFV contributions to a representative set of low-energy cLFV processes: $\mu \rightarrow e\gamma$, $\mu \rightarrow 3e$, and $\mu - e$ conversion in nuclei.

$\mu \rightarrow e\gamma$. The radiative decay $\mu \rightarrow e\gamma$ provides one of the strongest constraints on cLFV, with $\text{BR}(\mu \rightarrow e\gamma) < 4.2 \times 10^{-13}$ [95] and an expected order-of-magnitude improvement from MEG II [95, 96]. In the EFT framework, the dominant contribution arises from dipole operators of the form $\bar{\ell} \sigma^{\mu\nu} e$. Under extended MFV, the bilinear $\bar{\ell} e \sim \bar{\mathbf{3}}_\ell \otimes \mathbf{3}_e$ must be dressed with appropriate spurion insertions to form a flavor singlet. A single insertion of Y_e produces only flavor-aligned structures and does not induce cLFV. Off-diagonal transitions require additional spurions, with the leading contribution generated by $\Upsilon_\nu \Upsilon_\nu^\dagger Y_e$. Using the decomposition $\Upsilon_\nu \Upsilon_\nu^\dagger = \mathbf{1} \oplus \mathbf{8}_\ell \oplus \mathbf{27}_\ell$, the least-suppressed LFV invariant takes the form

$$\mathcal{I}_F^{\mu \rightarrow e\gamma} \sim \bar{\ell}_p [\Upsilon_\nu]^{ps} [\Upsilon_\nu^\dagger]_{st} [Y_e]^t{}_r e^r. \quad (\text{B1})$$

The induced dipole Wilson coefficient is therefore

$$[\mathcal{C}_{e\gamma}]^p{}_r = \frac{v}{\sqrt{2}} \frac{1}{\Lambda_{\text{LFV}}^2} [\Upsilon_\nu]^{ps} [\Upsilon_\nu^\dagger]_{st} [Y_e]^t{}_r, \quad (\text{B2})$$

with Λ_{LFV} the characteristic LFV scale. Inserting the spurion parametrization outlined in App. A, the resulting branching ratio scales as

$$\text{BR}(\mu \rightarrow 3e) \approx \mathcal{N}_\nu^{(1)} \times \left(\frac{\Lambda_L}{\Lambda_{\text{LFV}}} \right)^4 \times 10^{-50}, \quad (\text{B3})$$

where $\mathcal{N}_\nu^{(1)} \approx 90$ (30) for the case of NO (IO). Saturating the experimental bound yields

$$\left. \frac{\Lambda_L}{\Lambda_{\text{LFV}}} \right|_{\text{NO}} \lesssim 8 \times 10^8, \quad \left. \frac{\Lambda_L}{\Lambda_{\text{LFV}}} \right|_{\text{IO}} \lesssim 10 \times 10^8. \quad (\text{B4})$$

$\mu \rightarrow 3e$. The three-body decay $\mu \rightarrow 3e$ probes a broader set of effective interactions in comparison to $\mu \rightarrow e\gamma$. Besides dipole operators, this process receives direct contributions from four-fermion contact operators, as well as the operators contributing to the corrections to the gauge boson vertices. The current bound is $\text{BR}(\mu \rightarrow 3e) < 1.0 \times 10^{-12}$ [97], with future experiments such as Mu3e aiming to improve this sensitivity by several orders of magnitude [98].

In MFV, the relevant contributions can be classified according to the flavor structure of the lepton bilinear that induces the transition. For instance, the $\bar{\ell}\gamma_\mu\ell$ bilinear contains an adjoint of $U(3)_\ell$ in the decomposition, so the least-suppressed MFV invariant is obtained from $\Upsilon_\nu \Upsilon_\nu^\dagger \supset 8\ell$, implying a suppression of order $\mathcal{O}(\Upsilon_\nu^2)$. An analogous construction applies to $\bar{e}\gamma_\mu e$ bilinear. Since Υ_ν transforms as a $U(3)_e$ singlet, the leading invariant requires both Y_e^\dagger and Y_e , producing an overall suppression $\mathcal{O}(Y_e^2\Upsilon_\nu^2)$. For dipole operators, the leading MFV invariant is $Y_e \Upsilon_\nu \Upsilon_\nu^\dagger$, however, as in $\mu \rightarrow e\gamma$, the effective scaling of the branching ratio is ultimately controlled by Υ_ν^2 due to the cancellation of the explicit chiral factor in $\text{BR}(\mu \rightarrow 3e)$.

After inserting the spurion parametrization, the branch-

ing ratio takes the form

$$\text{BR}(\mu \rightarrow 3e) \approx \mathcal{N}_\nu^{(2)} \times \left(\frac{\Lambda_L}{\Lambda_{\text{LFV}}} \right)^4 \times 10^{-51}, \quad (\text{B5})$$

where $\mathcal{N}_\nu^{(2)} \approx 2$ (50) for NO (IO). Imposing the experimental limit yields

$$\left. \frac{\Lambda_L}{\Lambda_{\text{LFV}}} \right|_{\text{NO}} \lesssim 5 \times 10^9, \quad \left. \frac{\Lambda_L}{\Lambda_{\text{LFV}}} \right|_{\text{IO}} \lesssim 2 \times 10^9. \quad (\text{B6})$$

$\text{CR}(\mu - e, \mathbf{N})$. Unlike the purely leptonic processes $\mu \rightarrow e\gamma$ and $\mu \rightarrow 3e$, $\mu - e$ conversion is mediated by effective interactions involving both leptonic and quark currents. These include the vector-type, scalar-type as well as the dipole operators [99, 100]. The current bound from SINDRUM II [101] is $\text{CR}(\mu - e, \text{Au}) < 7.0 \times 10^{-13}$, with Mu2e [102] and COMET [103] expected to improve sensitivity down to $\mathcal{O}(10^{-17})$. As in the $\mu \rightarrow 3e$ case, the contributing SMEFT structures can be grouped according to the lepton bilinear, leading to the same MFV spurion power counting.

The resulting conversion rate in gold can be written as

$$\text{CR}(\mu - e, \text{Au}) \approx \mathcal{N}_\nu^{(3)} \times \left(\frac{\Lambda_L}{\Lambda_{\text{LFV}}} \right)^4 \times 10^{-50}, \quad (\text{B7})$$

where $\mathcal{N}_\nu^{(3)} \approx 10$ (4) for the case of NO (IO). Lastly, for the ratio of Λ_L and Λ_{LFV} scales we obtain

$$\left. \frac{\Lambda_L}{\Lambda_{\text{LFV}}} \right|_{\text{NO}} \lesssim 10 \times 10^8, \quad \left. \frac{\Lambda_L}{\Lambda_{\text{LFV}}} \right|_{\text{IO}} \lesssim 10 \times 10^8. \quad (\text{B8})$$

[1] G. D'Ambrosio, G. F. Giudice, G. Isidori and A. Strumia, *Minimal flavor violation: An Effective field theory approach*, *Nucl. Phys. B* **645** (2002) 155–187, [[hep-ph/0207036](#)].

[2] R. S. Chivukula and H. Georgi, *Composite Technicolor Standard Model*, *Phys. Lett. B* **188** (1987) 99–104.

[3] V. Cirigliano, B. Grinstein, G. Isidori and M. B. Wise, *Minimal flavor violation in the lepton sector*, *Nucl. Phys. B* **728** (2005) 121–134, [[hep-ph/0507001](#)].

[4] S. Davidson and F. Palorini, *Various definitions of Minimal Flavour Violation for Leptons*, *Phys. Lett. B* **642** (2006) 72–80, [[hep-ph/0607329](#)].

[5] R. Alonso, G. Isidori, L. Merlo, L. A. Munoz and E. Nardi, *Minimal flavour violation extensions of the seesaw*, *JHEP* **06** (2011) 037, [[1103.5461](#)].

[6] M. B. Gavela, T. Hambye, D. Hernandez and P. Hernandez, *Minimal Flavour Seesaw Models*, *JHEP* **09** (2009) 038, [[0906.1461](#)].

[7] P. Minkowski, $\mu \rightarrow e\gamma$ at a Rate of One Out of 10^9 Muon Decays?, *Phys. Lett. B* **67** (1977) 421–428.

[8] R. N. Mohapatra and G. Senjanovic, *Neutrino Masses and Mixings in Gauge Models with Spontaneous Parity Violation*, *Phys. Rev. D* **23** (1981) 165.

[9] R. Foot, H. Lew, X. G. He and G. C. Joshi, *Seesaw Neutrino Masses Induced by a Triplet of Leptons*, *Z. Phys. C* **44** (1989) 441.

[10] S. Davidson and S. Descotes-Genon, *Minimal Flavour Violation for Leptoquarks*, *JHEP* **11** (2010) 073, [[1009.1998](#)].

[11] E. Nikolidakis and C. Smith, *Minimal Flavor Violation, Seesaw, and R-parity*, *Phys. Rev. D* **77** (2008) 015021, [[0710.3129](#)].

[12] C. Smith, *Proton stability from a fourth family*, *Phys. Rev. D* **85** (2012) 036005, [[1105.1723](#)].

[13] A. Helset and A. Kobach, *Baryon Number, Lepton Number, and Operator Dimension in the SMEFT with Flavor Symmetries*, *Phys. Lett. B* **800** (2020) 135132, [[1909.05853](#)].

[14] S. Weinberg, *Baryon and Lepton Nonconserving Processes*, *Phys. Rev. Lett.* **43** (1979) 1566–1570.

[15] F. Wilczek and A. Zee, *Operator Analysis of Nucleon Decay*, *Phys. Rev. Lett.* **43** (1979) 1571–1573.

[16] L. F. Abbott and M. B. Wise, *The Effective Hamiltonian for Nucleon Decay*, *Phys. Rev. D* **22**

(1980) 2208.

[17] S. Weinberg, *Varieties of Baryon and Lepton Nonconservation*, *Phys. Rev. D* **22** (1980) 1694.

[18] SUPER-KAMIOKANDE collaboration, A. Takenaka et al., *Search for proton decay via $p \rightarrow e^+ \pi^0$ and $p \rightarrow \mu^+ \pi^0$ with an enlarged fiducial volume in Super-Kamiokande I-IV*, *Phys. Rev. D* **102** (2020) 112011, [[2010.16098](#)].

[19] SUPER-KAMIOKANDE collaboration, K. Abe et al., *Search for Nucleon Decay via $n \rightarrow \bar{\nu} \pi^0$ and $p \rightarrow \bar{\nu} \pi^+$ in Super-Kamiokande*, *Phys. Rev. Lett.* **113** (2014) 121802, [[1305.4391](#)].

[20] SUPER-KAMIOKANDE collaboration, R. Matsumoto et al., *Search for proton decay via $p \rightarrow \mu^+ K^0$ in 0.37 megaton-years exposure of Super-Kamiokande*, *Phys. Rev. D* **106** (2022) 072003, [[2208.13188](#)].

[21] HYPER-KAMIOKANDE collaboration, K. Abe et al., *Hyper-Kamiokande Design Report*, [1805.04163](#).

[22] DUNE collaboration, B. Abi et al., *Deep Underground Neutrino Experiment (DUNE), Far Detector Technical Design Report, Volume II: DUNE Physics*, [2002.03005](#).

[23] B. Grzadkowski, M. Iskrzynski, M. Misiak and J. Rosiek, *Dimension-Six Terms in the Standard Model Lagrangian*, *JHEP* **10** (2010) 085, [[1008.4884](#)].

[24] W. Buchmuller and D. Wyler, *Effective Lagrangian Analysis of New Interactions and Flavor Conservation*, *Nucl. Phys. B* **268** (1986) 621–653.

[25] A. B. Beneito, I. J. Gargalionis, J. Herrero-Garcia, A. Santamaria and M. A. Schmidt, *An EFT approach to baryon number violation: lower limits on the new physics scale and correlations between nucleon decay modes*, *JHEP* **07** (2024) 004, [[2312.13361](#)].

[26] CMS collaboration, A. Hayrapetyan et al., *Search for baryon number violation in top quark production and decay using proton-proton collisions at $\sqrt{s} = 13$ TeV*, *Phys. Rev. Lett.* **132** (2024) 241802, [[2402.18461](#)].

[27] BABAR collaboration, P. del Amo Sanchez et al., *Searches for the baryon- and lepton-number violating decays $B^0 \rightarrow \Lambda_c^+ \ell^-$, $B^- \rightarrow \Lambda \ell^-$, and $B^- \rightarrow \bar{\Lambda} \ell^-$* , *Phys. Rev. D* **83** (2011) 091101, [[1101.3830](#)].

[28] LHCb collaboration, R. Aaij et al., *Search for the baryon- and lepton-number violating decays $B0 \rightarrow p\mu^-$ and $Bs0 \rightarrow p\mu^-$* , *Phys. Rev. D* **108** (2023) 012021, [[2210.10412](#)].

[29] W.-S. Hou, M. Nagashima and A. Soddu, *Baryon number violation involving higher generations*, *Phys. Rev. D* **72** (2005) 095001, [[hep-ph/0509006](#)].

[30] M. Beneke, G. Finauri and A. A. Petrov, *Indirect constraints on third generation baryon number violation*, *JHEP* **09** (2024) 090, [[2404.09642](#)].

[31] A. Crivellin and M. Hoferichter, *Rescattering effects in nucleon-to-meson form factors and application to tau-lepton-induced proton decay*, *Phys. Lett. B* **845** (2023) 138169, [[2302.01939](#)].

[32] H. Gisbert, A. Rodríguez-Sánchez and L. Vale Silva, *Constraints on baryon-number-violating top-quark operators in standard model effective field theory*, *Phys. Rev. D* **112** (2025) 015026, [[2409.00218](#)].

[33] J. Heeck and D. Watkins, *Baryon number violation involving tau leptons*, *JHEP* **07** (2024) 170, [[2405.18478](#)].

[34] Z. Dong, G. Durieux, J.-M. Gerard, T. Han and F. Maltoni, *Baryon number violation at the LHC: the top option*, *Phys. Rev. D* **85** (2012) 016006, [[1107.3805](#)].

[35] W. J. Marciano, *Tau physics: A Theoretical perspective*, *Nucl. Phys. B Proc. Suppl.* **40** (1995) 3–15.

[36] M. Thomas Arun, S. M and R. Pal, *RG evolution and effect of intermediate new-physics on $\Delta B = 1$ four-fermion operators*, [2511.06106](#).

[37] R. Barbieri, G. Isidori, J. Jones-Perez, P. Lodone and D. M. Straub, *$U(2)$ and Minimal Flavour Violation in Supersymmetry*, *Eur. Phys. J. C* **71** (2011) 1725, [[1105.2296](#)].

[38] G. Isidori and D. M. Straub, *Minimal Flavour Violation and Beyond*, *Eur. Phys. J. C* **72** (2012) 2103, [[1202.0464](#)].

[39] R. Barbieri, D. Buttazzo, F. Sala and D. M. Straub, *Flavour physics from an approximate $U(2)^3$ symmetry*, *JHEP* **07** (2012) 181, [[1203.4218](#)].

[40] L. Allwicher, C. Cornellà, G. Isidori and B. A. Stefanek, *New physics in the third generation. A comprehensive SMEFT analysis and future prospects*, *JHEP* **03** (2024) 049, [[2311.00020](#)].

[41] A. Greljo, A. Palavrić and A. E. Thomsen, *Adding Flavor to the SMEFT*, *JHEP* **10** (2022) 010, [[2203.09561](#)].

[42] A. Greljo and A. Palavrić, *Leading directions in the SMEFT*, *JHEP* **09** (2023) 009, [[2305.08898](#)].

[43] A. Greljo, A. Palavrić and A. Smolković, *Leading directions in the SMEFT: Renormalization effects*, *Phys. Rev. D* **109** (2024) 075033, [[2312.09179](#)].

[44] I. Esteban, M. C. Gonzalez-Garcia, M. Maltoni, I. Martinez-Soler, J. P. Pinheiro and T. Schwetz, *NuFit-6.0: updated global analysis of three-flavor neutrino oscillations*, *JHEP* **12** (2024) 216, [[2410.05380](#)].

[45] R. Alonso, H.-M. Chang, E. E. Jenkins, A. V. Manohar and B. Shotwell, *Renormalization group evolution of dimension-six baryon number violating operators*, *Phys. Lett. B* **734** (2014) 302–307, [[1405.0486](#)].

[46] A. B. I. Beneito, J. Gargalionis, J. Herrero-Garcia and M. A. Schmidt, *Squeezing Proton Decay and Neutrino Masses: Upper Bounds on Standard Model Extensions*, [2503.20928](#).

[47] I. Dorsner, S. Fajfer and N. Kosnik, *Heavy and light scalar leptoquarks in proton decay*, *Phys. Rev. D* **86** (2012) 015013, [[1204.0674](#)].

[48] P. Nath and P. Fileviez Perez, *Proton stability in grand unified theories, in strings and in branes*, *Phys. Rept.* **441** (2007) 191–317, [[hep-ph/0601023](#)].

[49] E. E. Jenkins, A. V. Manohar and P. Stoffer, *Low-Energy Effective Field Theory below the Electroweak Scale: Operators and Matching*, *JHEP* **03** (2018) 016, [[1709.04486](#)].

[50] PARTICLE DATA GROUP collaboration, S. Navas et al., *Review of particle physics*, *Phys. Rev. D* **110** (2024) 030001.

[51] M. Claudson, M. B. Wise and L. J. Hall, *Chiral Lagrangian for Deep Mine Physics*, *Nucl. Phys. B* **195** (1982) 297–307.

[52] J.-S. Yoo, Y. Aoki, P. Boyle, T. Izubuchi, A. Soni and S. Syritsyn, *Proton decay matrix elements on the lattice at physical pion mass*, *Phys. Rev. D* **105** (2022) 074501, [[2111.01608](#)].

[53] Y. Aoki, T. Izubuchi, E. Shintani and A. Soni, *Improved lattice computation of proton decay matrix*

elements, *Phys. Rev. D* **96** (2017) 014506, [[1705.01338](#)].

[54] RBC-UKQCD collaboration, Y. Aoki, P. Boyle, P. Cooney, L. Del Debbio, R. Kenway, C. M. Maynard et al., *Proton lifetime bounds from chirally symmetric lattice QCD*, *Phys. Rev. D* **78** (2008) 054505, [[0806.1031](#)].

[55] RQCD collaboration, G. S. Bali, S. Collins, W. Söldner and S. Weishäupl, *Leading order mesonic and baryonic $SU(3)$ low energy constants from $N_f=3$ lattice QCD*, *Phys. Rev. D* **105** (2022) 054516, [[2201.05591](#)].

[56] A. Celis, J. Fuentes-Martin, A. Vicente and J. Virto, *DsixTools: The Standard Model Effective Field Theory Toolkit*, *Eur. Phys. J. C* **77** (2017) 405, [[1704.04504](#)].

[57] J. Fuentes-Martin, P. Ruiz-Femenia, A. Vicente and J. Virto, *DsixTools 2.0: The Effective Field Theory Toolkit*, *Eur. Phys. J. C* **81** (2021) 167, [[2010.16341](#)].

[58] M. Magg and C. Wetterich, *Neutrino Mass Problem and Gauge Hierarchy*, *Phys. Lett. B* **94** (1980) 61–64.

[59] T. P. Cheng and L.-F. Li, *Neutrino Masses, Mixings and Oscillations in $SU(2) \times U(1)$ Models of Electroweak Interactions*, *Phys. Rev. D* **22** (1980) 2860.

[60] D. Wyler and L. Wolfenstein, *Massless Neutrinos in Left-Right Symmetric Models*, *Nucl. Phys. B* **218** (1983) 205–214.

[61] G. 't Hooft, C. Itzykson, A. Jaffe, H. Lehmann, P. K. Mitter, I. M. Singer et al., eds., *Recent Developments in Gauge Theories. Proceedings, Nato Advanced Study Institute, Cargese, France, August 26 - September 8, 1979*, vol. 59, 1980. 10.1007/978-1-4684-7571-5.

[62] J. de Blas, J. C. Criado, M. Perez-Victoria and J. Santiago, *Effective description of general extensions of the Standard Model: the complete tree-level dictionary*, *JHEP* **03** (2018) 109, [[1711.10391](#)].

[63] J. C. Helo, M. Hirsch and T. Ota, *Proton decay at one loop*, *Phys. Rev. D* **99** (2019) 095021, [[1904.00036](#)].

[64] J. Gargalionis, J. Herrero-García and M. A. Schmidt, *Model-independent estimates for loop-induced baryon-number-violating nucleon decays*, *JHEP* **06** (2024) 182, [[2401.04768](#)].

[65] I. Doršner, S. Fajfer, A. Greljo, J. F. Kamenik and N. Košnik, *Physics of leptoquarks in precision experiments and at particle colliders*, *Phys. Rept.* **641** (2016) 1–68, [[1603.04993](#)].

[66] A. Palavrić, *Discrete leptonic flavor symmetries: UV mediators and phenomenology*, *Phys. Rev. D* **110** (2024) 115025, [[2408.16044](#)].

[67] A. Moreno-Sánchez and A. Palavrić, *Leptonic Flavor from Modular A_4 : UV Mediators and SMEFT Realizations*, [2505.01535](#).

[68] R. Bartocci, A. Biekötter and T. Hurth, *A global analysis of the SMEFT under the minimal MFV assumption*, *JHEP* **05** (2024) 074, [[2311.04963](#)].

[69] L. Allwicher, M. McCullough and S. Renner, *New physics at Tera-Z: precision renormalised*, *JHEP* **02** (2025) 164, [[2408.03992](#)].

[70] J. ter Hoeve, L. Mantani, J. Rojo, A. N. Rossia and E. Vryonidou, *Connecting scales: RGE effects in the SMEFT at the LHC and future colliders*, *JHEP* **06** (2025) 125, [[2502.20453](#)].

[71] M. Papucci, J. T. Ruderman and A. Weiler, *Natural SUSY Endures*, *JHEP* **09** (2012) 035, [[1110.6926](#)].

[72] G. Larsen, Y. Nomura and H. L. L. Roberts, *Supersymmetry with Light Stops*, *JHEP* **06** (2012) 032, [[1202.6339](#)].

[73] R. Barbieri, D. Buttazzo, F. Sala, D. M. Straub and A. Tesi, *A 125 GeV composite Higgs boson versus flavour and electroweak precision tests*, *JHEP* **05** (2013) 069, [[1211.5085](#)].

[74] O. Matsedonskyi, *On Flavour and Naturalness of Composite Higgs Models*, *JHEP* **02** (2015) 154, [[1411.4638](#)].

[75] G. Panico and A. Pomarol, *Flavor hierarchies from dynamical scales*, *JHEP* **07** (2016) 097, [[1603.06609](#)].

[76] L. Allwicher, G. Isidori and A. E. Thomsen, *Stability of the Higgs Sector in a Flavor-Inspired Multi-Scale Model*, *JHEP* **01** (2021) 191, [[2011.01946](#)].

[77] J. Fuentes-Martin and P. Stangl, *Third-family quark-lepton unification with a fundamental composite Higgs*, *Phys. Lett. B* **811** (2020) 135953, [[2004.11376](#)].

[78] J. Fuentes-Martin, G. Isidori, J. M. Lizana, N. Selimovic and B. A. Stefanek, *Flavor hierarchies, flavor anomalies, and Higgs mass from a warped extra dimension*, *Phys. Lett. B* **834** (2022) 137382, [[2203.01952](#)].

[79] J. Fuentes-Martin and J. M. Lizana, *Deconstructing flavor anomalously*, *JHEP* **07** (2024) 117, [[2402.09507](#)].

[80] A. Greljo and B. A. Stefanek, *Third family quark-lepton unification at the TeV scale*, *Phys. Lett. B* **782** (2018) 131–138, [[1802.04274](#)].

[81] R. Barbieri and G. Isidori, *Minimal flavour deconstruction*, *JHEP* **05** (2024) 033, [[2312.14004](#)].

[82] R. Barbieri, *Phenomenology of Minimal Flavour Deconstruction at the lowest new scale*, [2409.08657](#).

[83] M. Bordone, C. Cornellà, J. Fuentes-Martin and G. Isidori, *A three-site gauge model for flavor hierarchies and flavor anomalies*, *Phys. Lett. B* **779** (2018) 317–323, [[1712.01368](#)].

[84] J. Davighi and B. A. Stefanek, *Deconstructed hypercharge: a natural model of flavour*, *JHEP* **11** (2023) 100, [[2305.16280](#)].

[85] J. Davighi and G. Isidori, *Non-universal gauge interactions addressing the inescapable link between Higgs and flavour*, *JHEP* **07** (2023) 147, [[2303.01520](#)].

[86] S. Covone, J. Davighi, G. Isidori and M. Pesut, *Flavour deconstructing the composite Higgs*, *JHEP* **01** (2025) 041, [[2407.10950](#)].

[87] J. M. Lizana, *A common origin of the Higgs boson and the flavor hierarchies*, *JHEP* **05** (2025) 176, [[2412.14243](#)].

[88] M. Fernández Navarro and S. F. King, *Tri-hypercharge: a separate gauged weak hypercharge for each fermion family as the origin of flavour*, *JHEP* **08** (2023) 020, [[2305.07690](#)].

[89] M. Fernández Navarro, S. F. King and A. Vicente, *Minimal complete tri-hypercharge theories of flavour*, *JHEP* **07** (2024) 147, [[2404.12442](#)].

[90] M. Fernández Navarro, S. F. King and A. Vicente, *Natural neutrino mass hierarchy in a theory of gauge flavour deconstruction*, [2506.21687](#).

[91] G. Isidori, P. Paradisi, A. Sainaghi and N. Selimovic, *Anarchic neutrinos from flavor deconstruction: phenomenology of the lepton sector*, [2510.23703](#).

[92] A. Greljo, A. Palavrić and B. A. Stefanek, *Minimal Flavor Protection for TeV-scale New Physics*, [2512.04159](#).

[93] R. M. Fonseca, *The Sym2Int program: going from symmetries to interactions*, *J. Phys. Conf. Ser.* **873** (2017) 012045, [[1703.05221](#)].

[94] R. M. Fonseca, *Enumerating the operators of an effective field theory*, *Phys. Rev. D* **101** (2020) 035040, [[1907.12584](#)].

[95] MEG collaboration, A. M. Baldini et al., *Search for the lepton flavour violating decay $\mu^+ \rightarrow e^+ \gamma$ with the full dataset of the MEG experiment*, *Eur. Phys. J. C* **76** (2016) 434, [[1605.05081](#)].

[96] MEG II collaboration, A. M. Baldini et al., *The design of the MEG II experiment*, *Eur. Phys. J. C* **78** (2018) 380, [[1801.04688](#)].

[97] SINDRUM collaboration, U. Bellgardt et al., *Search for the Decay $\mu^+ \rightarrow e^+ e^+ e^-$* , *Nucl. Phys. B* **299** (1988) 1–6.

[98] A. Blondel et al., *Research Proposal for an Experiment to Search for the Decay $\mu \rightarrow eee$* , [1301.6113](#).

[99] M. Raidal and A. Santamaria, *Muon electron conversion in nuclei versus mu $\rightarrow e$ gamma: An Effective field theory point of view*, *Phys. Lett. B* **421** (1998) 250–258, [[hep-ph/9710389](#)].

[100] L. Calibbi, X. Marcano and J. Roy, *Z lepton flavour violation as a probe for new physics at future $e^+ e^-$ colliders*, *Eur. Phys. J. C* **81** (2021) 1054, [[2107.10273](#)].

[101] SINDRUM II collaboration, W. H. Bertl et al., *A Search for muon to electron conversion in muonic gold*, *Eur. Phys. J. C* **47** (2006) 337–346.

[102] Mu2E collaboration, L. Bartoszek et al., *Mu2e Technical Design Report*, [1501.05241](#).

[103] COMET collaboration, Y. Fujii, *A search for a muon to electron conversion in COMET*, *JINST* **18** (2023) C10010, [[2308.14275](#)].